

# El Niño MODOKI\*\*\*

*\*\*\*In Press, JGR-Oceans*

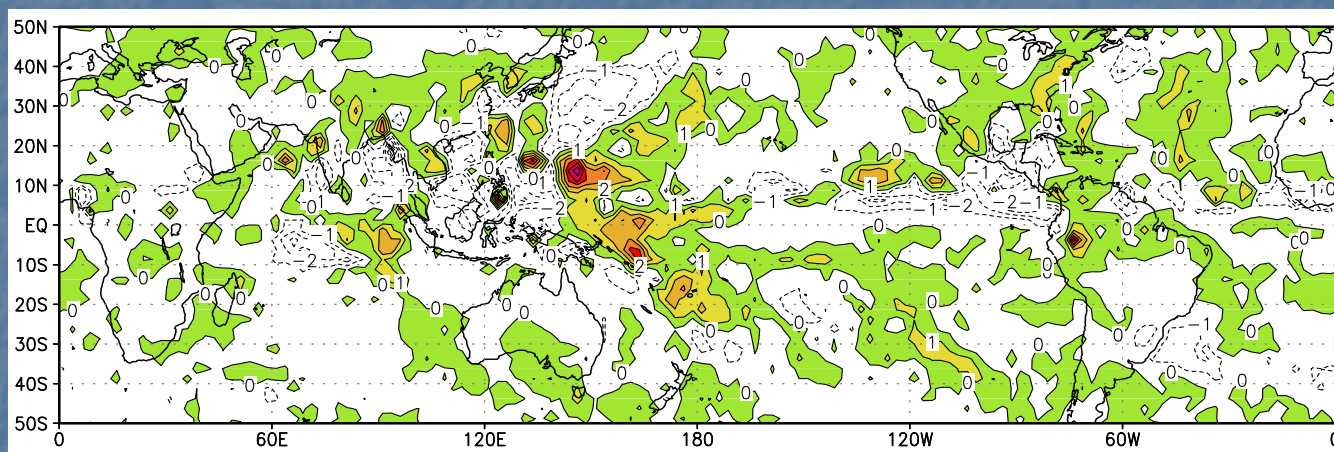
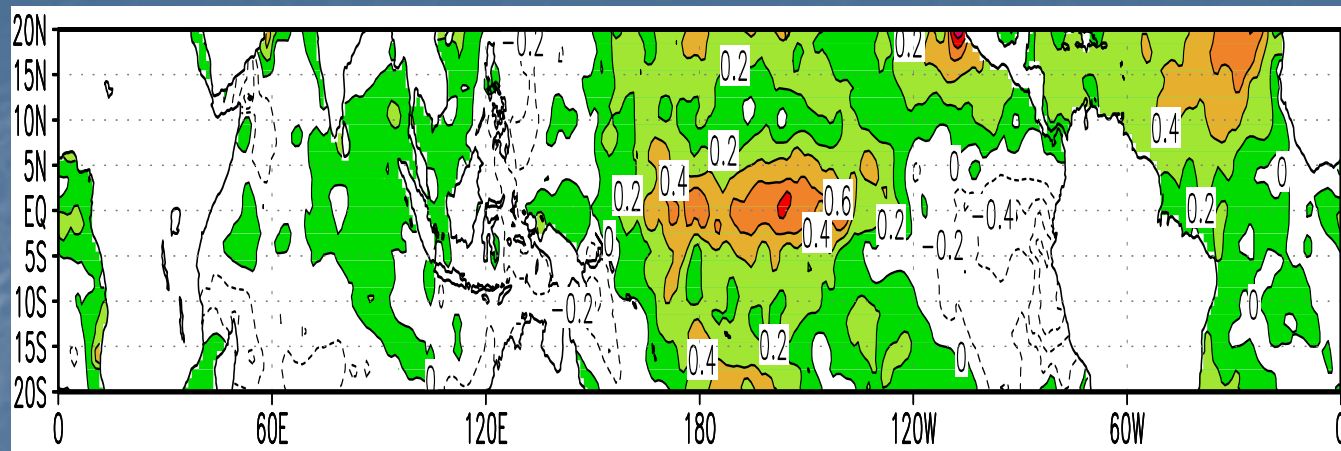
# Division of the talk

- El Niño Modoki – a tropical Pacific mode independent from ENSO.
- Involves coupled processes – coupled mode
- Teleconnection
- Decadal variability and background state
- Summary

# Datasets

*(mainly for the Period 1979-2005feb)*

- HadISST (Rayner et al., 2003)  
*Verification by OISST (Reynolds, 2002) from 1982*
- GPCP Precipitation (Adler et al., 2003)  
*Verification by CMAP precipitation (Xie and Arkin, 1996)*
- NCEP/NCAR reanalysis (Kalnay et al., 1996)  
*Verification by ERA40 (Simmons and Gibson, 2000)*
- SODA (Carton et al., 2005; Carton and Giese, 2006).
- Also Levitus data, Aviso data, QUICKSCAT data etc.



Top: Anomalous JJAS 2004 SST (°C).  
 Bottom: Anomalous JJAS 2004 rainfall (cm/month)

# Rationale for classification as a new phenomenon

- El Niño (Rasmusson and Carpenter type)? – No
- Also does not fit the so called “Date line El Niño” (NOAA definition /Larkin and Harrison, 2005 GRL) that is only based on warming in NINO3.4 region *irrespective of warming/cooling in eastern tropical Pacific*.
- We call it **El Niño Modoki**. This word was introduced by Prof. Yamagata during 2004 while explaining a probable cause behind the abnormal summer climatic conditions over Japan. It has been often used since then by various Japanese Mass Media. “Modoki” is a classical Japanese word which means “similar but different”.

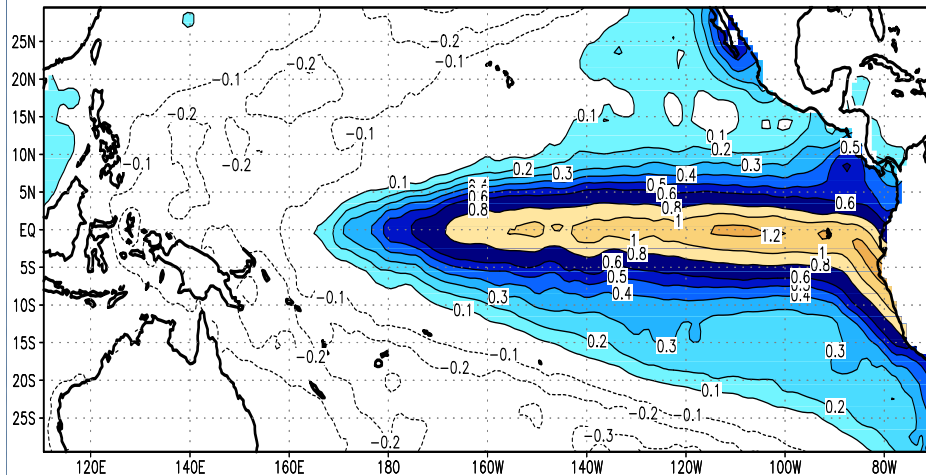
# Methodology

- EOF analysis
- Varimax analysis
- Composite analysis
- Partial correlation analysis
- Difference of long term means to understand the recent occurrence of persistent and frequent Modoki events

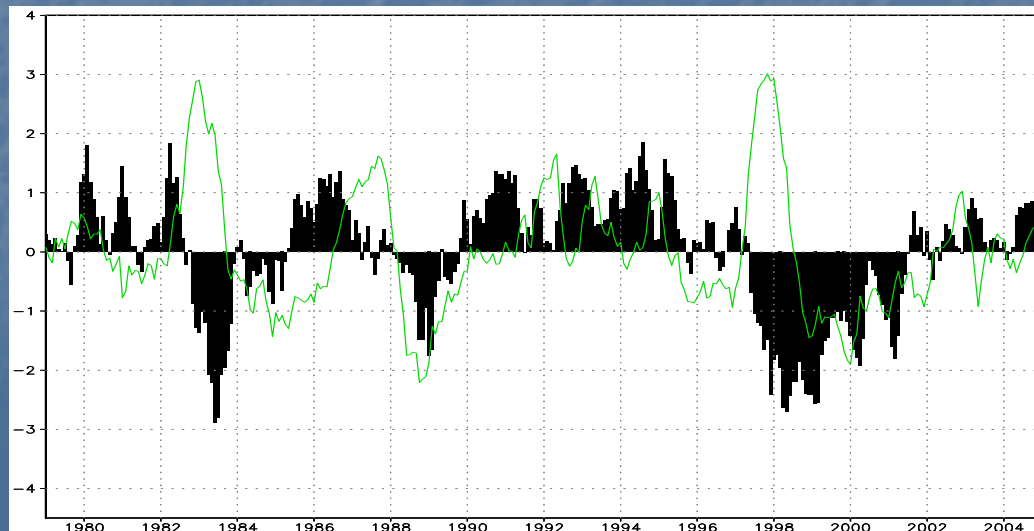
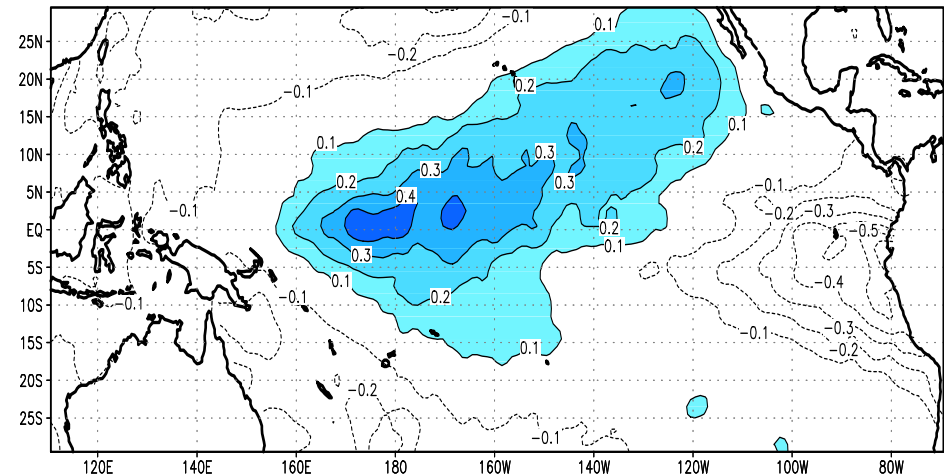
# Methodology

- EOF analysis
- Varimax analysis
- Composite analysis
- Partial correlation analysis
- Difference of long term means to understand the recent occurrence of persistent and frequent Modoki events

(a) EOF1 (HadISSTA from 1979–2004; 45%)

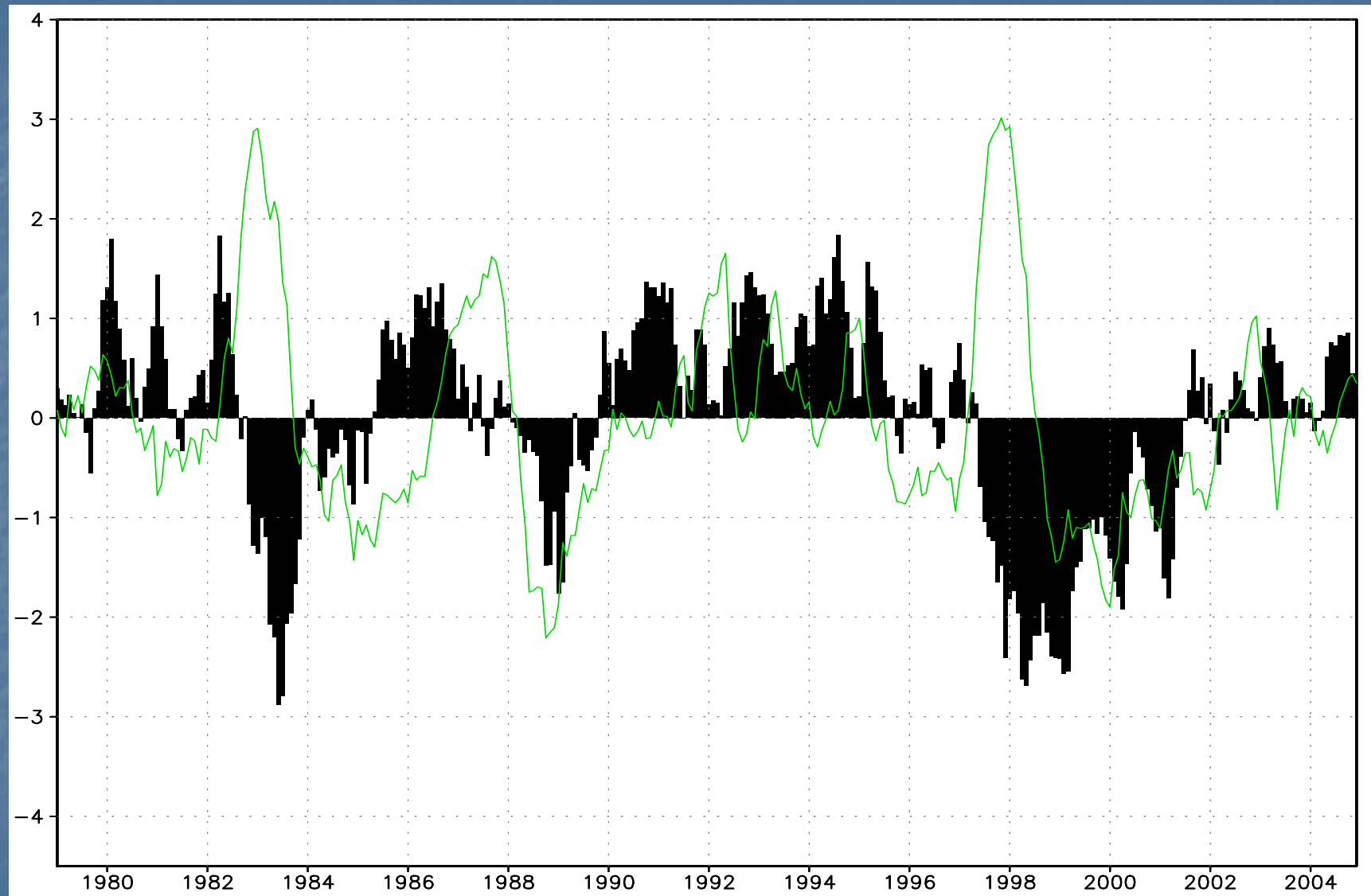


(b) EOF2 (HadISSTA from 1979–2004; 12%)



Above: Top two EOF modes of tropical Pacific SSTA (1979–2005 Feb.) multiplied by respective standard deviations of the principal components; units in  $^{\circ}\text{C}$ .

Right: Normalized time series of PC1 (green line) and PC2 (Bar).



## Correlations with PC2

NINO3 index	-0.09
NINO4 index	0.51
NINO1+2 index	-0.44
NINO3.4 index	0.19
IODMI	0.1
SDMI	0.15

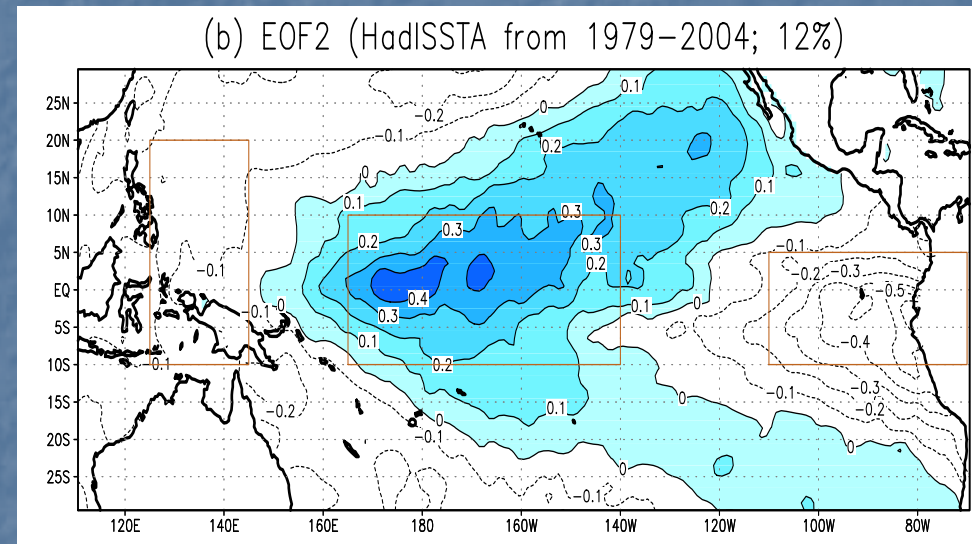
Even the magnitude of the maximum lead-Lag correlations between the PC1 and PC2 after 1978 is a modest 0.43, indicating that more than 80% of either of the phenomenon is independent of the other.

# An index for El Niño Modoki

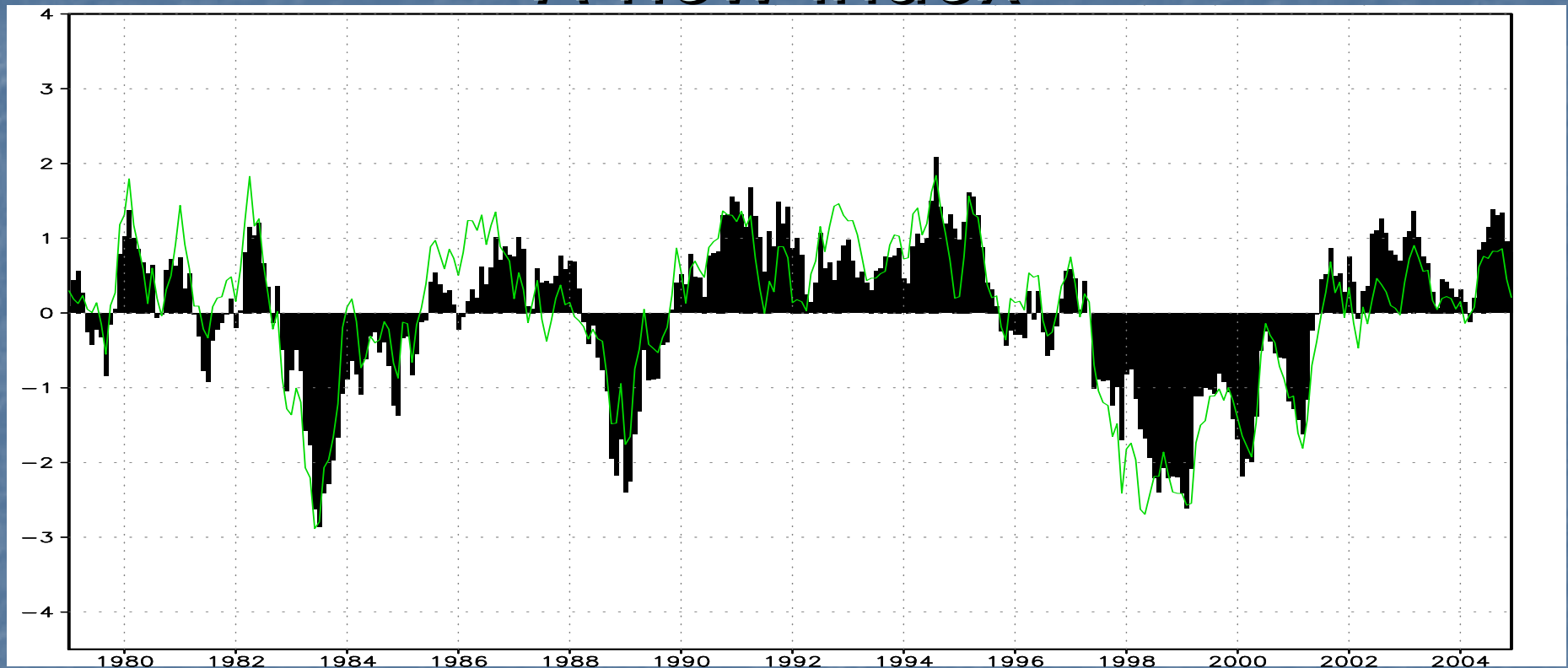
- Based on the EOF2 pattern, we derive an El Niño Modoki index (EMI). Because of the unique tripolar nature of the SSTA, the index, from SSTA, is derived as follows:

$$\text{EMI} = A - 0.5 * B - 0.5 * C$$

where 'A, B, and C' are the are-averaged SSTA over Central tropical Pacific (165E-140W, 10S-10N), Eastern tropical Pacific (110W-70W, 15S-5N), and Western tropical Pacific (125E-145E, 10S-20N).



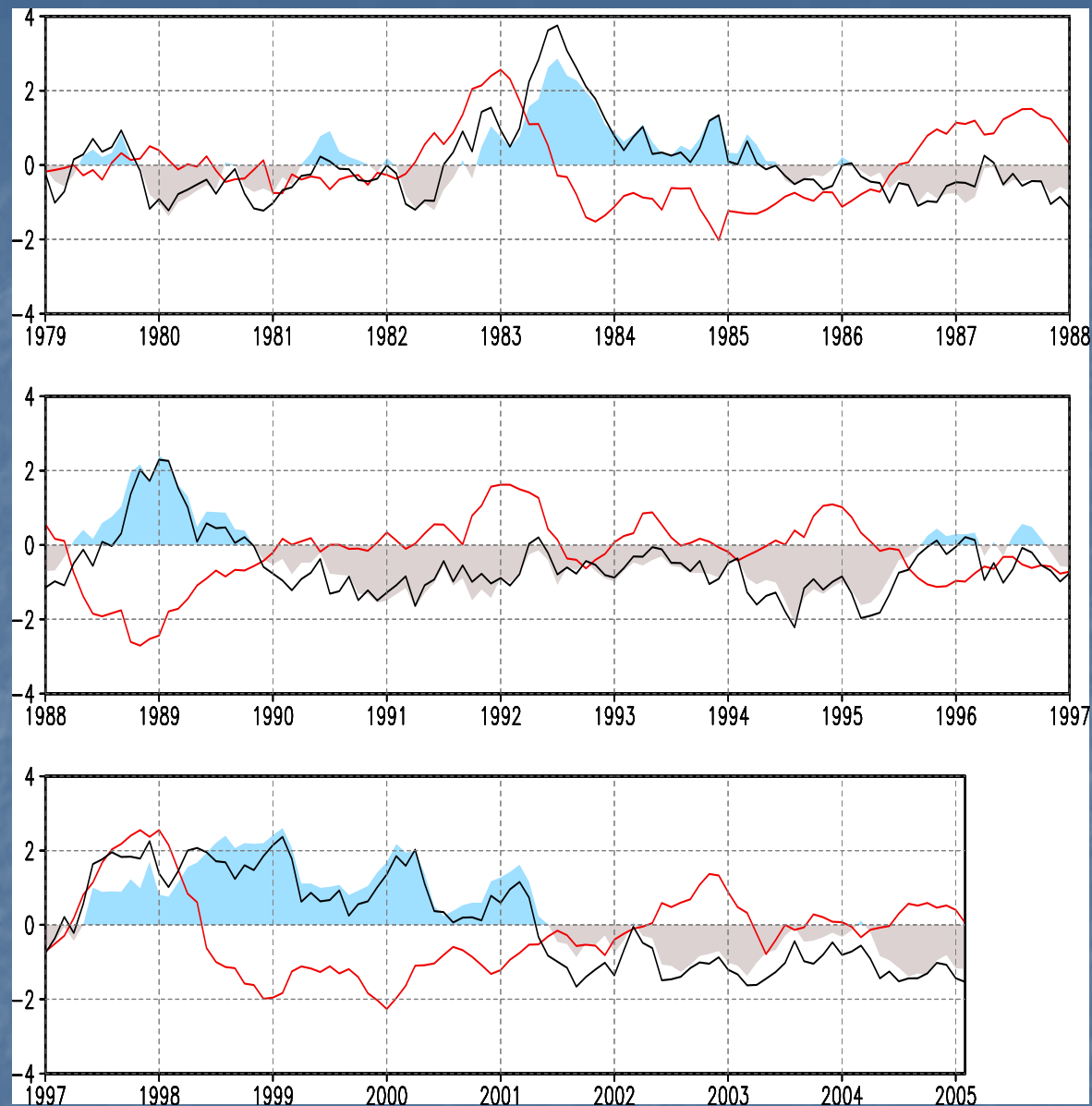
# A new index



**Top: Time series of normalized ENSO Modoki index (EMI; in bar) and that of the PC2 (green line). The standard deviation of the EMI is  $0.52^{\circ}\text{C}$ . The correlation with PC2 for the period 1979-2005Feb. is 0.92.**

# EMI vs. TNI

- Trenberth and Stepaniak (2001) introduced another index called trans-Nino index (TNI) as the difference between normalized SSTA between NINO4 and NINO1+2. TNI is correlated at 0.8 with the time series of SVD2 of SSTA and several atmospheric fields such as precipitation (Trenberth et al., 2002), and hence they accept TNI as an index to represent the SVD2 in tropical pacific; The correlation of the SVD2 time series with tropical pacific SSTA resembles that of our EOF2.
- The correlation between TNI and EMI is -0.87 for the study period. From this simple analysis, TNI appears to be almost the same as EMI. Nevertheless, we will show the advantage of EMI in the following.

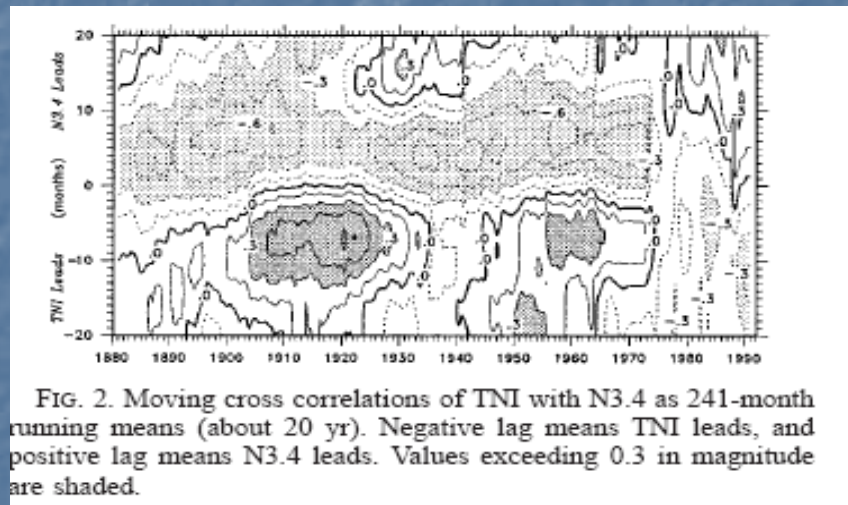


The time series of normalized Nino3.4 (red line) index, and TNI (blue line) as defined by Trenberth and Stepaniak (2001). Also shown is the time series of the *inverted* EMI (shaded). The sign of the EMI has been deliberately reversed in this figure to facilitate easy comparison of its evolution with the TNI.

- The correlations of the PC2 with NINO4 and NINO1+2 indices are 0.51 and -0.44 respectively. On the other hand, its correlations with SSTA in our equivalent boxes in the central and eastern tropical Pacific are 0.51 and -0.42. Up to that, both indices are similar.
- However, most interestingly, the correlation of the PC2 with our western box (B) is -0.45, stronger in amplitude than that with NINO1+2, the eastern box of SSTA defining the TNI. This demonstrates that the western tropical Pacific SSTA is just as important as that of the eastern Pacific.

- We consider that the EMI is better statistically as well as dynamically to represent the EOF2 pattern of tropical Pacific SSTA variability. The relative correlations of EMI and TNI with PC2 are 0.93 and 0.88, elucidating the slight superiority of EMI. However, because of their strong similarity and association with EOF2, both indices may be considered analogous in representation of the El Niño Modoki for many practical purposes, just as the NINO3 and NINO3.4 indices in case of El Niño events.

# Relationship between ENSO and ENSO Modoki



Trenberth and Stepaniak (2001) indicate that NINO3.4 and TNI are significantly correlated at different lags/leads, and hence they conclude that their SVD2 pattern is one phase of ENSO evolution. However, they admit that the relationship has changed along with changes in ENSO characteristics after the climate regime shift in the middle 1970s (Nitta and Yamada, 1989). It is seen in their Fig. 2 that the lag/lead moving correlations have considerably weakened after 1976; these also changed their respective signs. Hence, their conjecture that the El Niño Modoki pattern of SSTA is part of El Niño evolution is not always supported.

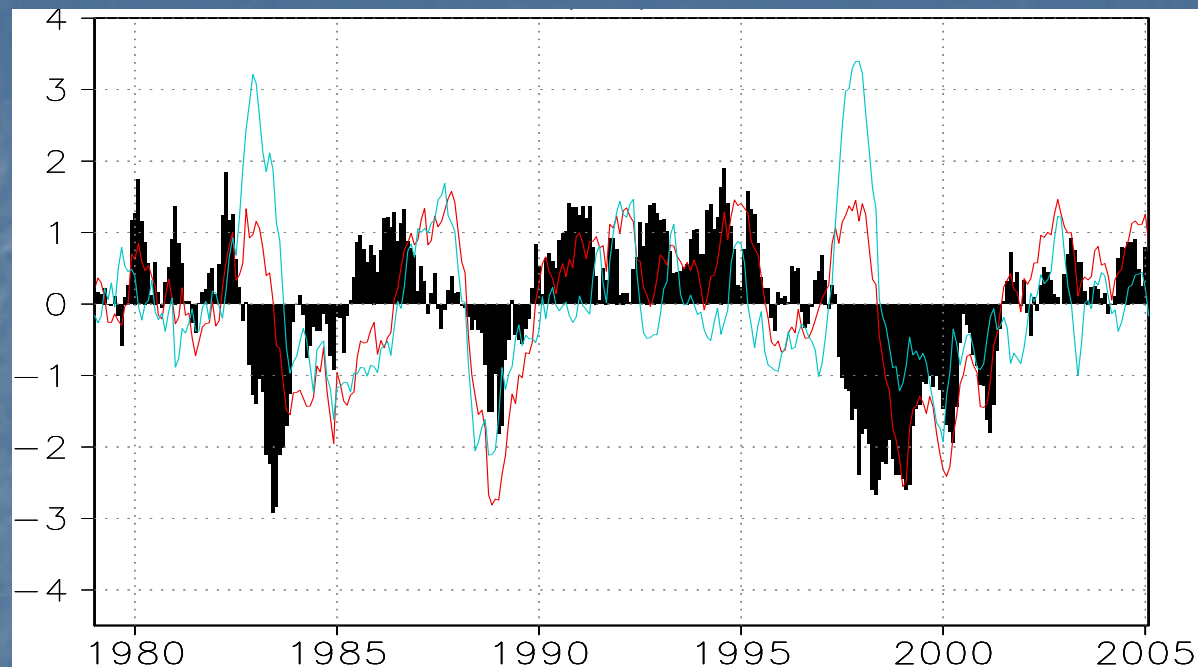


*Fig (above). Normalized time series of the PC2 (principal component of the EOF2) of tropical Pacific SST variability (Bar), NINO3 SSTA (blue) and Nino4 indices (red).*

If the hypothesis of Trenberth and Stepaniak (2001) applies, the El Niño Modoki conditions in summer of 2004 should have been followed (preceded) by an El Niño (a La Niña) after (before) 3-12 months; ***neither of these things happened, as indicated by the NINO3.4 index (or by the NINO3 index).***

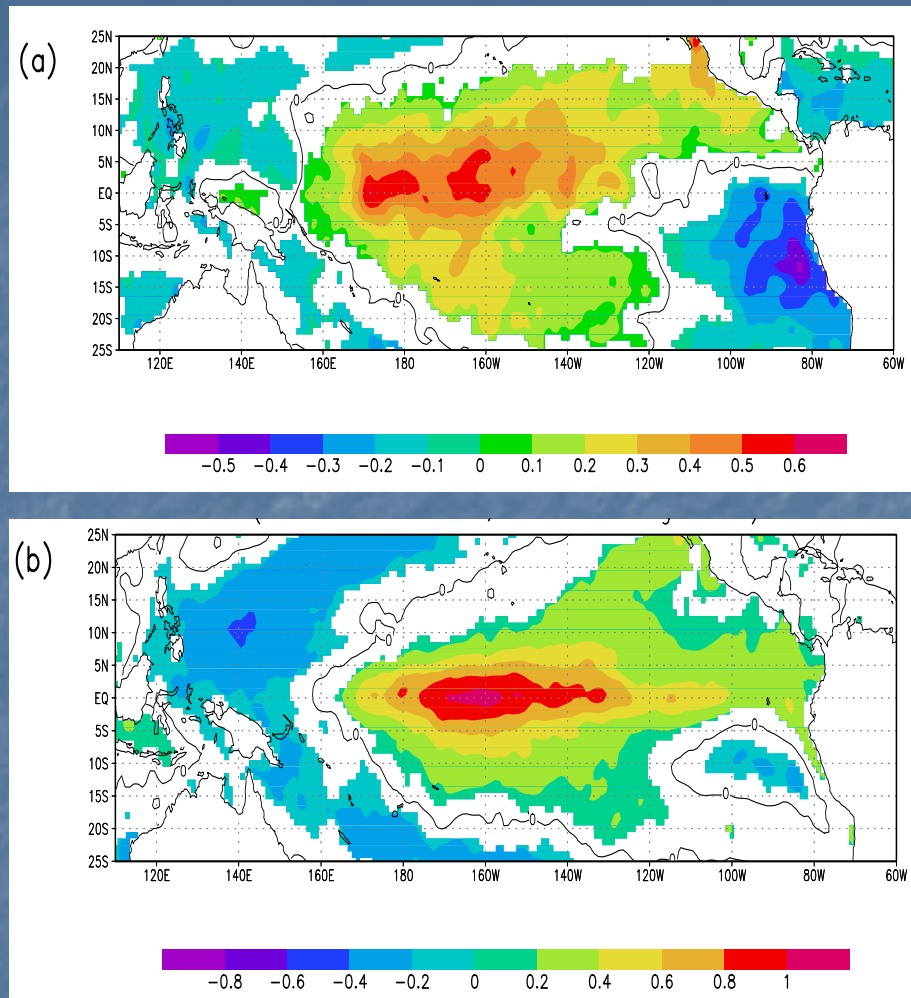
- In fact, out of the three major El Niño events after 1977, only the 1982-83 period fits the hypothesis stipulated by Trenberth and Stepaniak (2001). Even during 1997 when a strong El Niño event occurred, it was preceded by a very weak El Niño Modoki event. Importantly, it can also be seen that the condition suggested by Trenberth and Stepaniak (2001) is not valid for the so-called protracted El Niño period of 1990-94.

- To further understand the relationship between El Niño Modoki and El Niño, a lead-lag analysis between the monthly values of the EMI and NINO3 index was carried out for the study period. It has turned out that EMI between April and October is correlated ( $>0.45$ ) with NINO3 index in December. On the other hand, February NINO3 index leads the August EMI with correlation of about 0.5. Similarly, Nino 3.4 index correlated (0.49) with EMI at 4 months lag. All these indicate that, after 1978, *only up to a maximum of 30%* of the total variance of either one of the El Niño Modoki and El Niño phenomena can be explained by the other.

# Composite Analysis

- Based on the time series of the EMI shown in Fig. 4a, we have identified seven strong [\[1\]](#) El Niño Modoki events that lasted from boreal summer through boreal winter, peaking in one of these seasons (seasonal standard deviations for boreal summer and winter are  $0.5^{\circ}\text{C}$  and  $0.54^{\circ}\text{C}$  respectively). These strong El Niño Modoki events occurred in 1986, 1990, 1991, 1992, 1994, 2002, and 2004. Additionally, we identified a strong El Niño Modoki during the boreal winter of 1979-80 that lasted through the summer of 1980, though its amplitude fell below the threshold of  $0.7\sigma$  by then.

\*\*\*\*\*[\[1\]](#) We define a strong El Niño Modoki event when its amplitude of the index is equal to or greater than  $0.7\sigma$ , where  $\sigma$  is the seasonal standard deviation.



Composite SSTA in  $^{\circ}\text{C}$  during strong positive El Niño Modoki events averaged over (a) seven boreal summers, namely JJAS seasons of 1986, 1990, 1991, 1992, 1994, 2002 and 2004 and (b) 8 boreal winters, namely DJF seasons of 1979-80, 1986-87, 1990-91, 1991-92, 1992-93, 1994-95, 2002-2003 and 2004-05. Significant values above 95% confidence level from a two tailed Student's t-test are shaded.

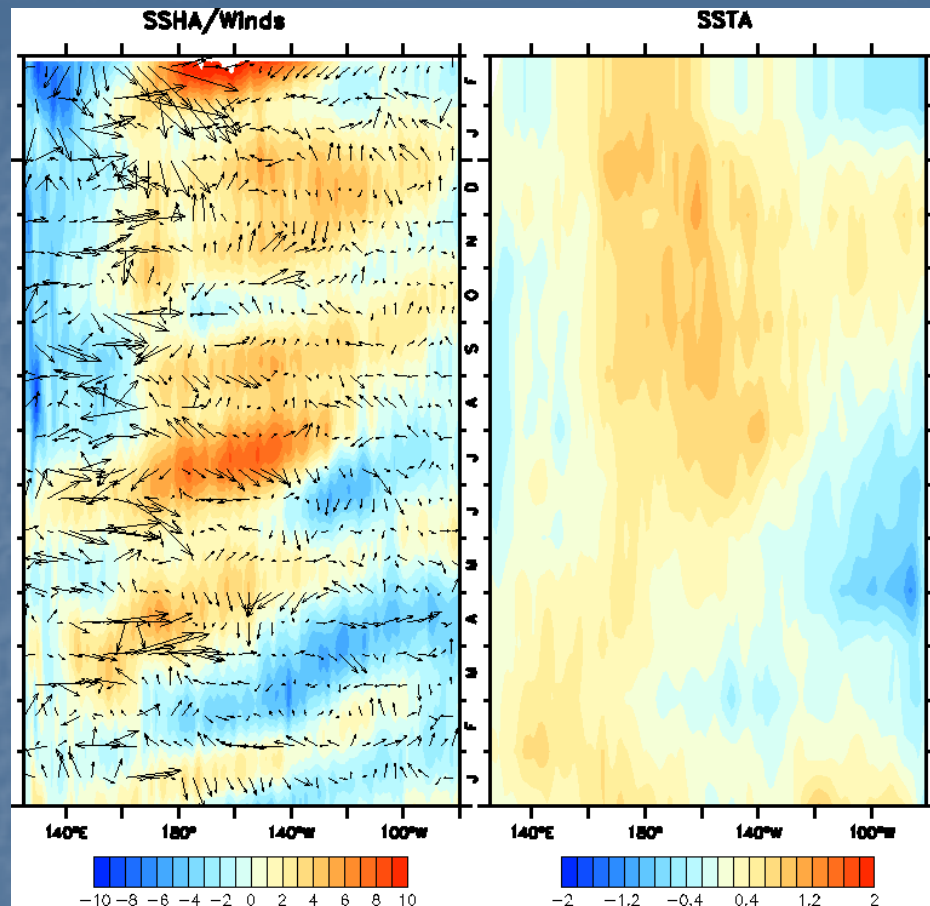
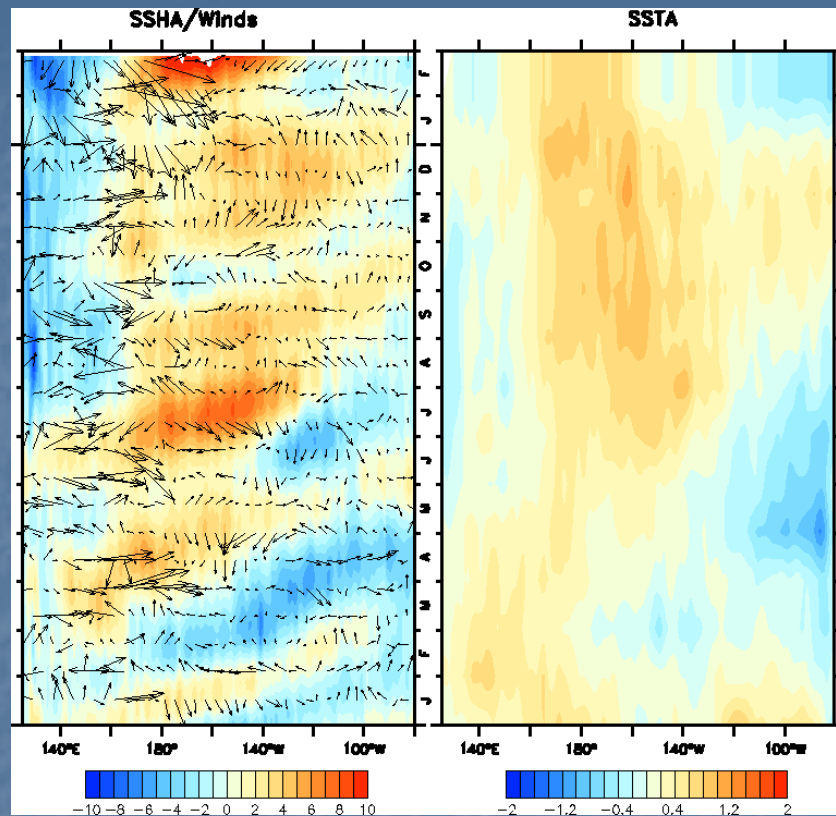
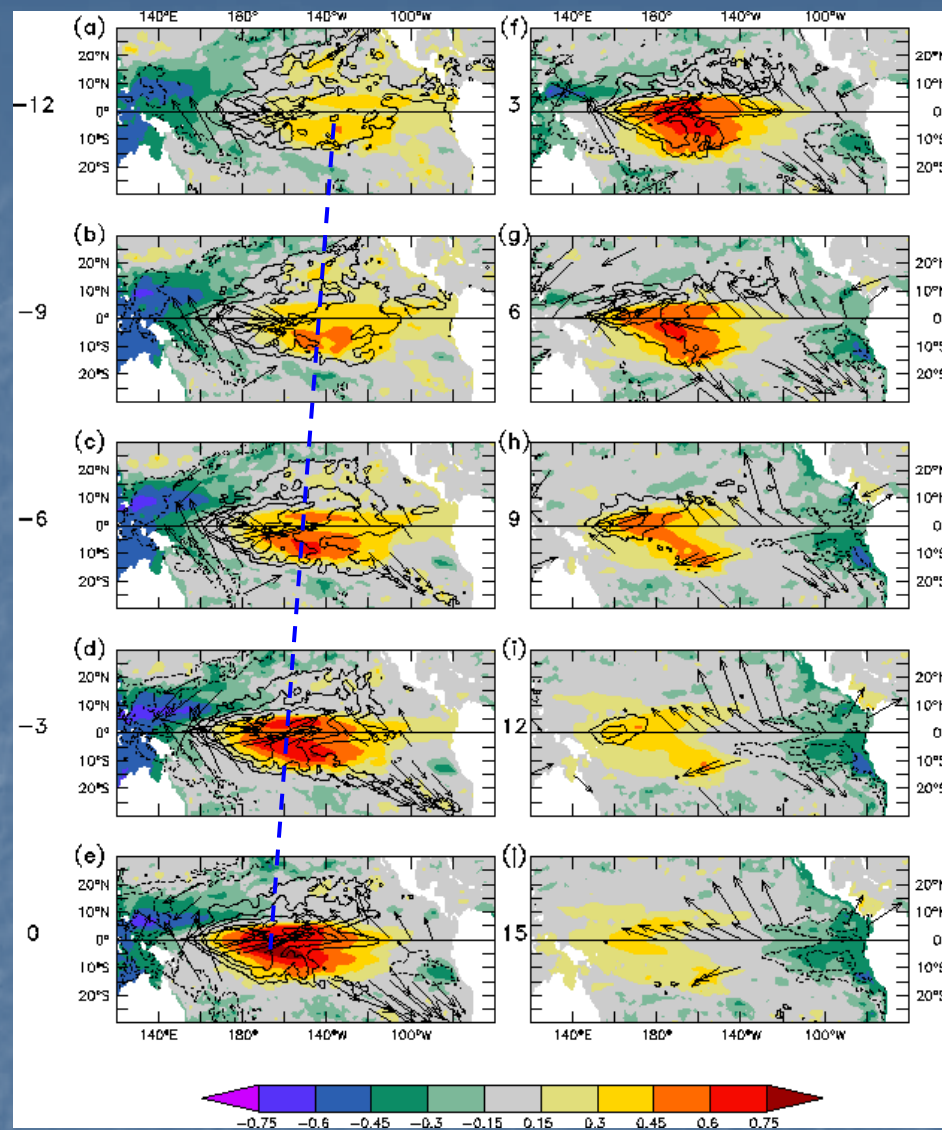


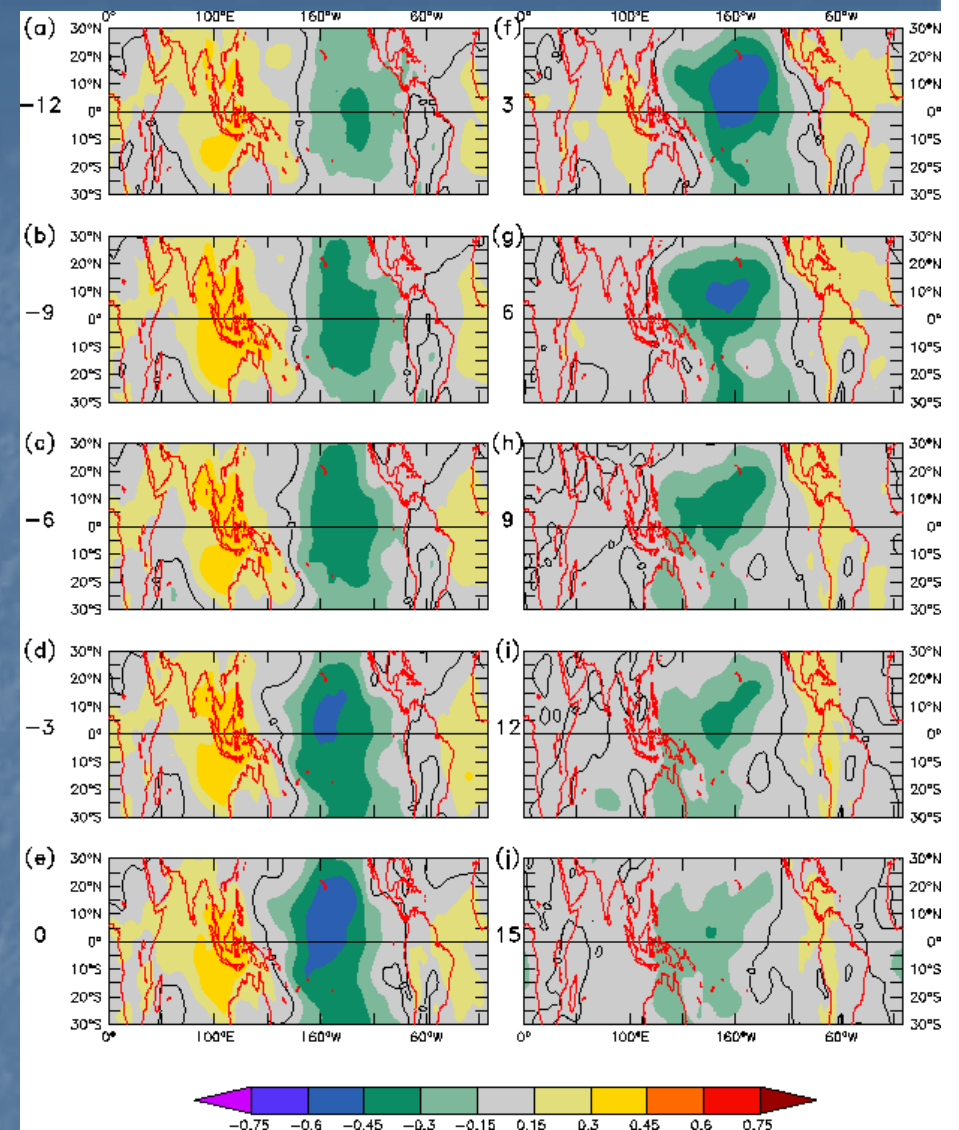
**Figure** Abnormal conditions during JJA in 2004: (a) SSTA in °C (b) evolution of SSHA in cm (shaded) and wind anomalies (m.s-1; vectors), averaged between 2°S-2°N, and (c) evolution of SSTA averaged between 5°S-5° N. (Aviso SSHA, Quikscat winds, and HadiSSTA)



- the ENSO Modoki events are triggered from tropical Western Pacific.
- Because of this importance of western tropical pacific, it is also worth noticing that the correlation of the western tropical Pacific SSTA with EMI is -0.51, much higher in magnitude than the correlation of 0.25 with TNI.



**(Left):** Lag/lead correlations of monthly EMI with sea surface height anomalies (shading) and ocean temperature anomalies at 10 meter depth (contours). Positive (negative) correlation coefficients correspond to rise (fall) of sea level. Regressed winds with EMI are shown only if the correlation coefficient between EMI and respective wind components exceeds 0.15 (significant at 90% confidence level from a 2-tailed Student's t-test). Lag/lead values in months are shown on the left hand side of each plot.



**(Right):** Lag/lead correlations of monthly EMI with SLPA.

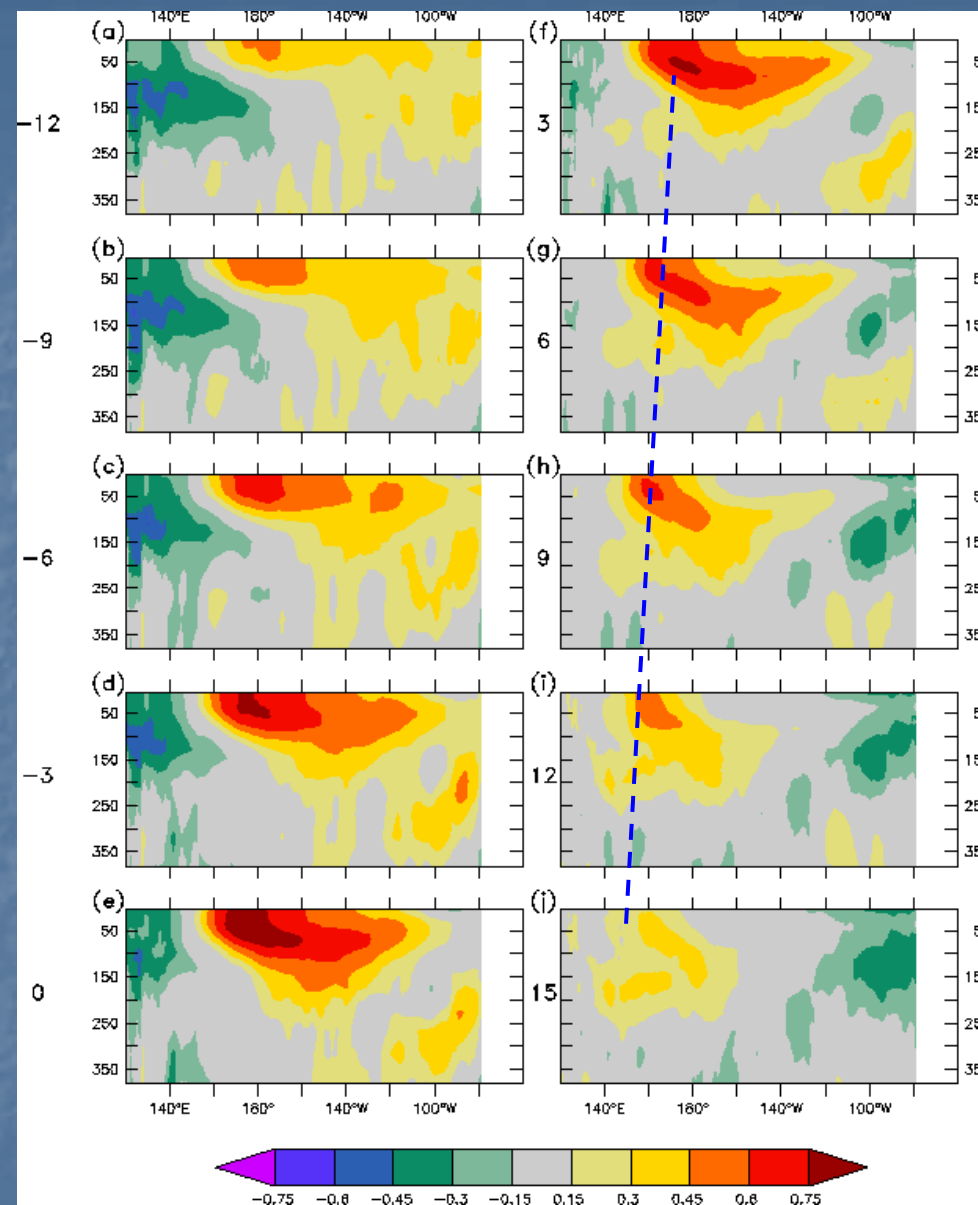


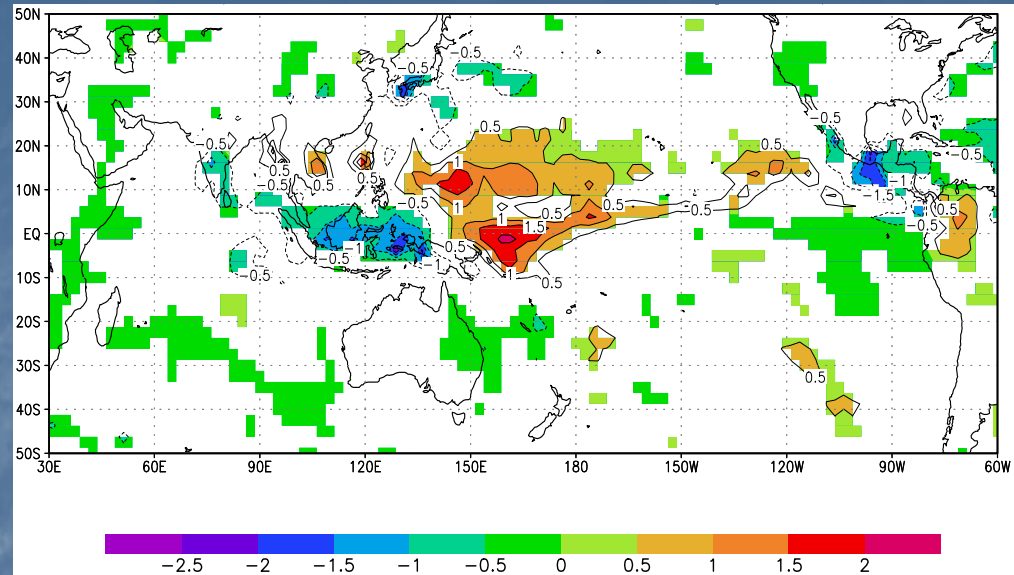
Fig. Lag/lead correlations of EMI with ocean subsurface temperature anomalies at different depths in meters averaged over 2°S–2°N.

Lag/lead values in months are shown on the left hand side of each plot.

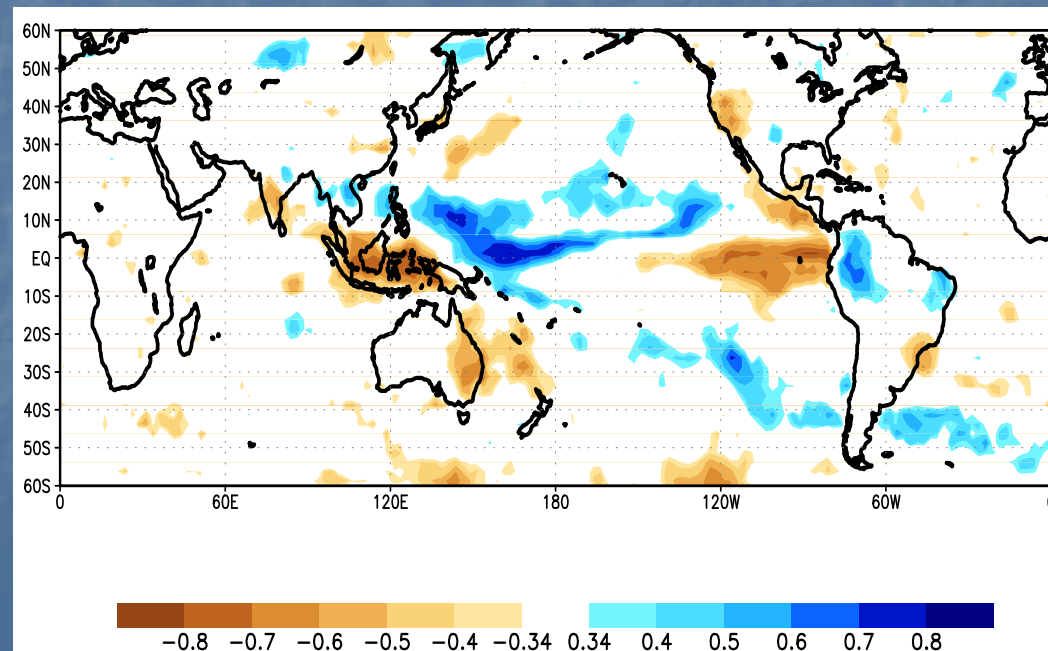
# The reason for the lag/lead correlations

- The significant lead/lag correlations between the indices of ENSO and ENSO Modoki discussed earlier can be attributed to the fact that the tropical central Pacific is the common playground for both of these phenomena. Nevertheless, the magnitude of these correlations is relatively modest. This is because of the difference in the zonal extent of this playground for the coupled dynamics during these two phenomena. During El Niño events in years such as 1982-83 and 1997-98, the equatorial central Pacific warming propagates to the tropical eastern Pacific. However, during majority of the El Niño Modoki events, the propagation takes place only up to the equatorial Central Pacific.

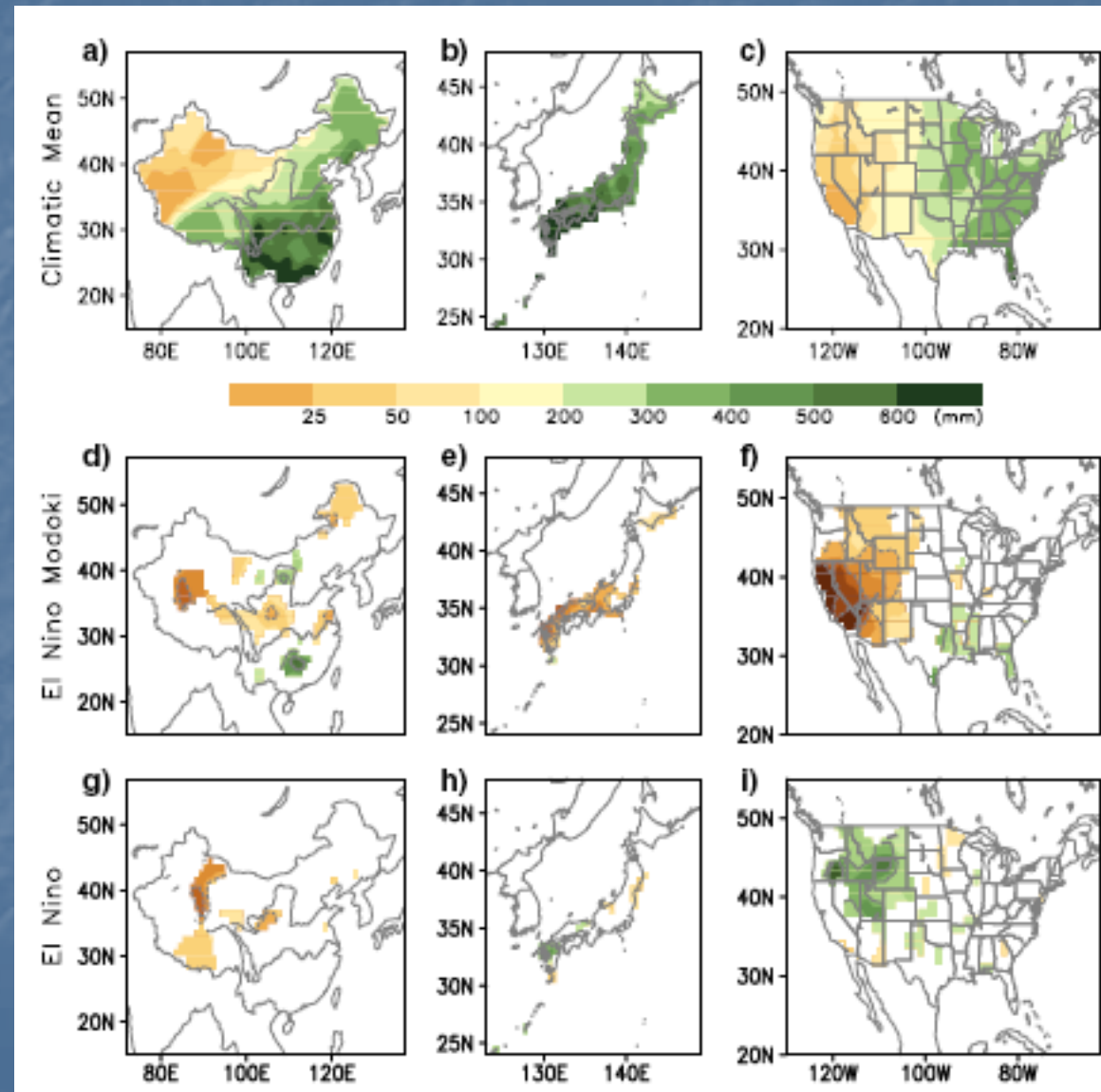
# TELECONNECTIONS

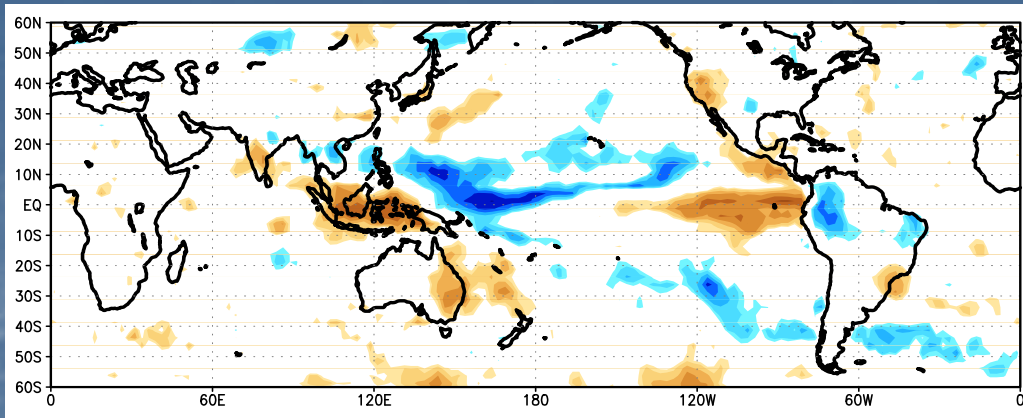


**(top)** Composite JJAS GPCP rainfall anomalies (cm/month) during strong positive El Niño Modoki events averaged over seven boreal summers. **(below)** Partial Corr. of GPCP rainfall With EMI.



## Impacts of Modoki and ENSO corroborated by the station data



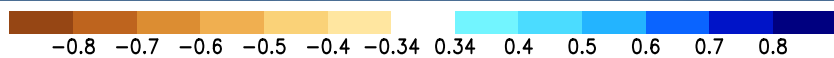
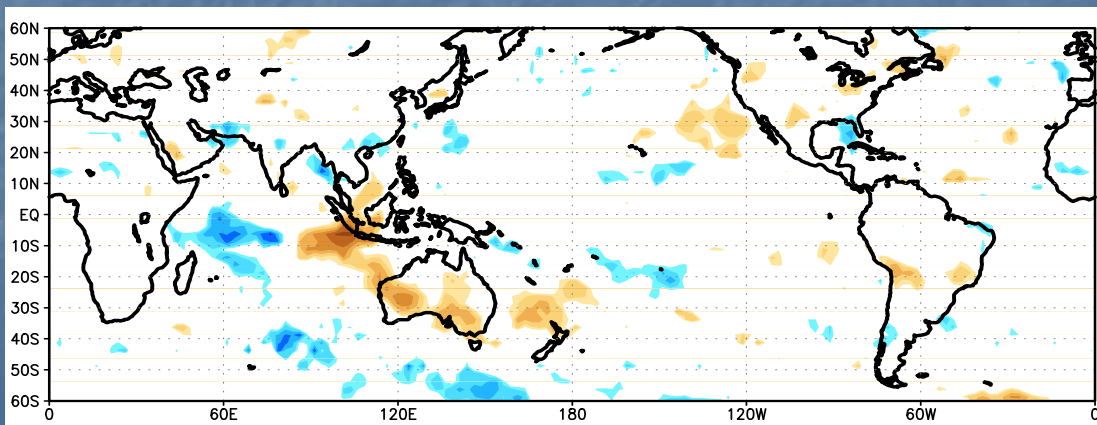
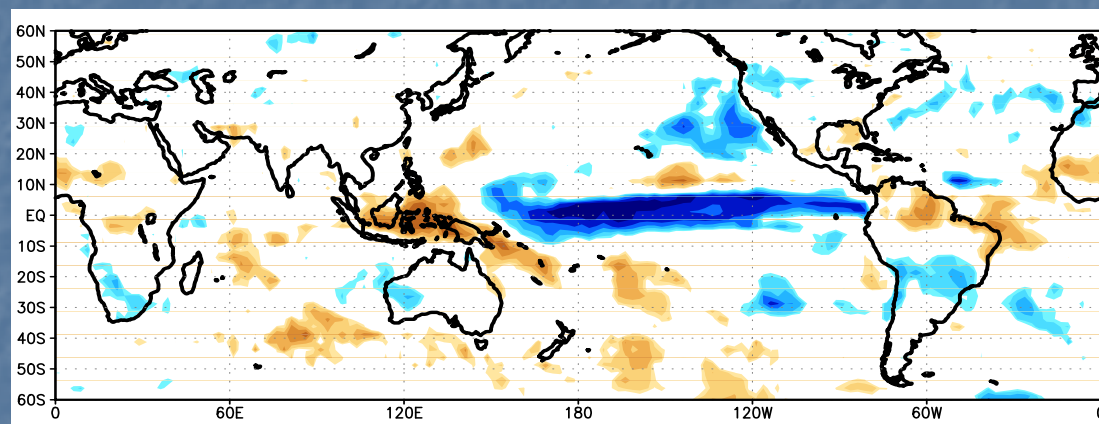


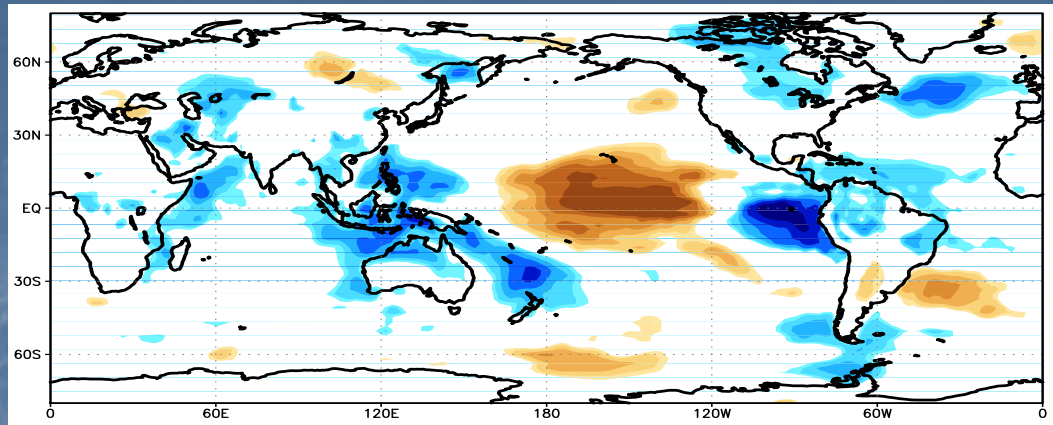
JJAS Partial Corr. of GPCP  
rainfall With

EMI

NINO3

IODMI



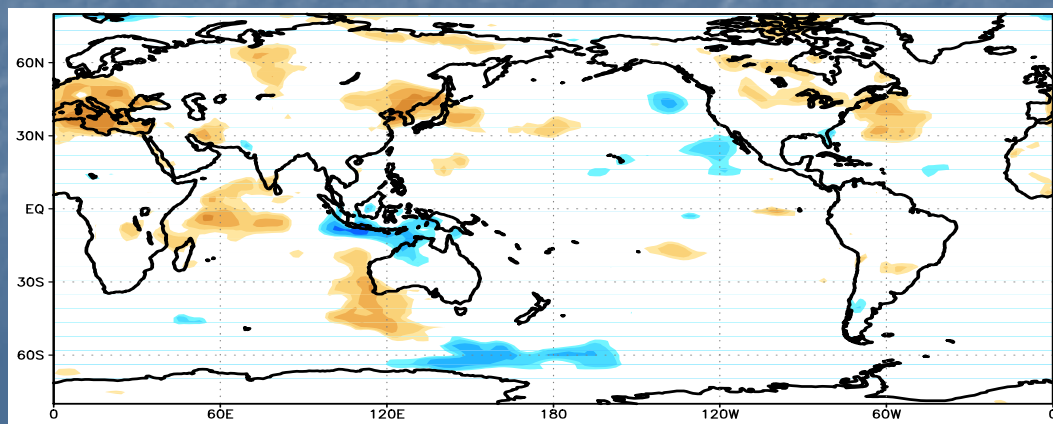
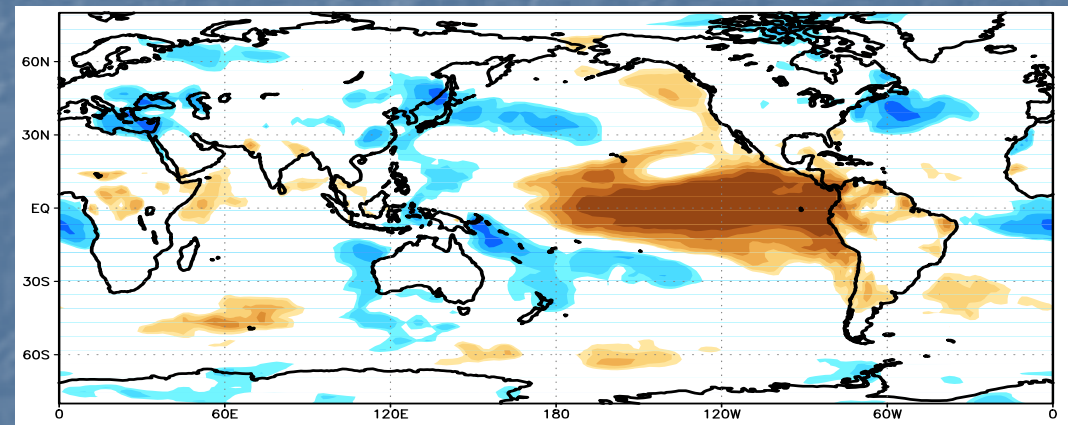


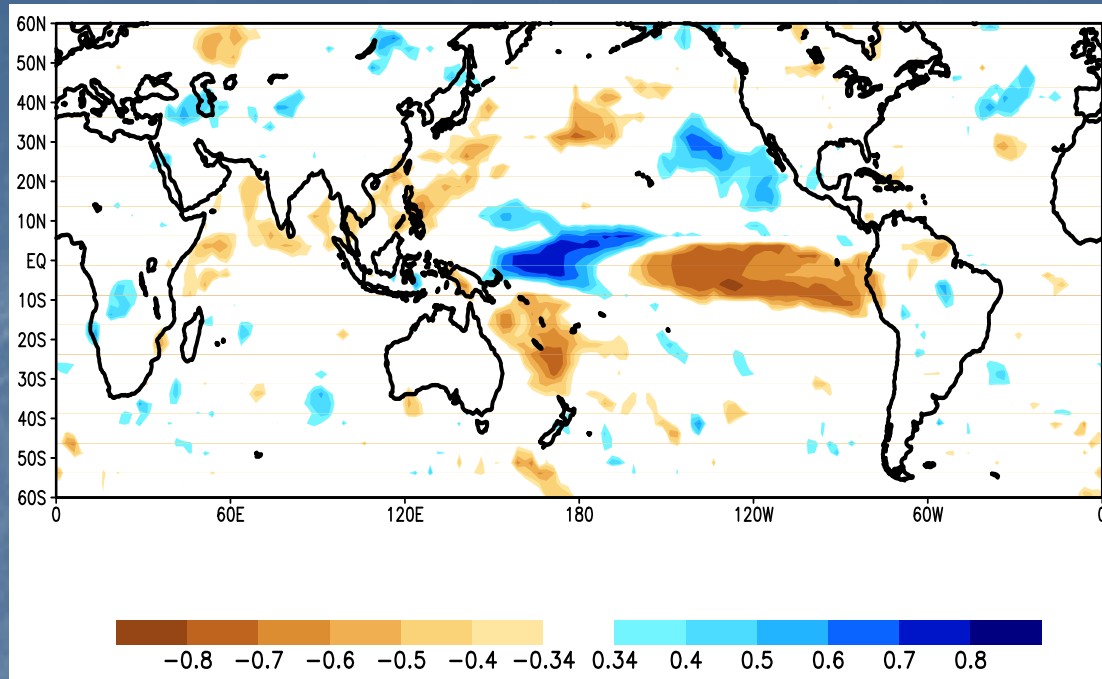
JJAS Partial Corr. of surface  
temperature With

EMI

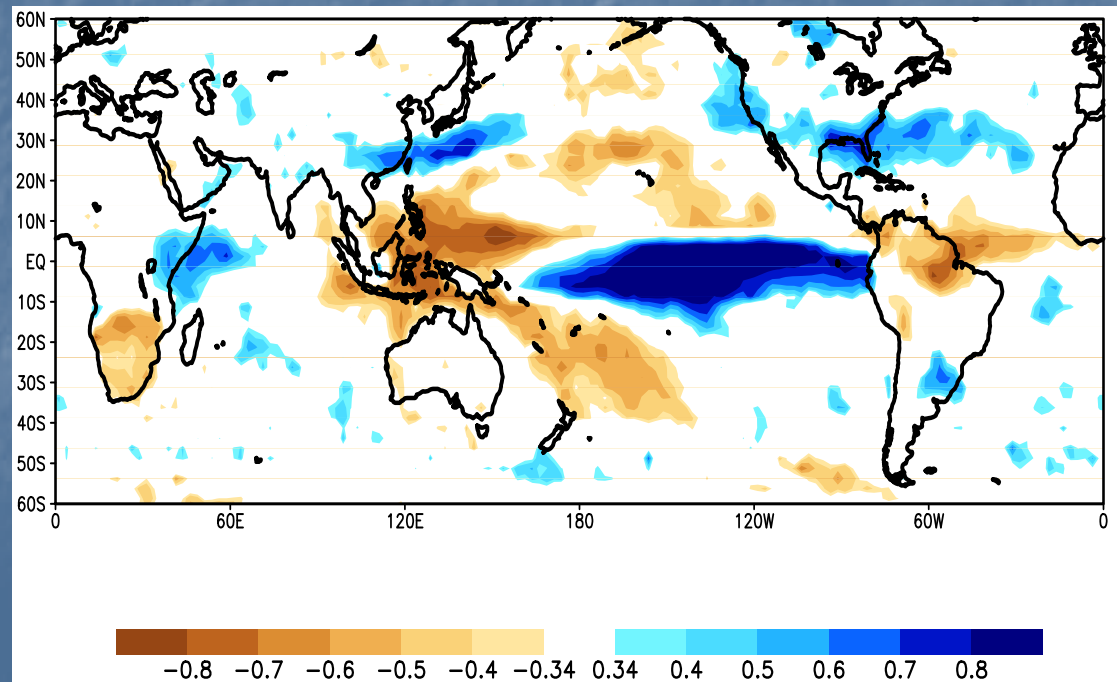
NINO3

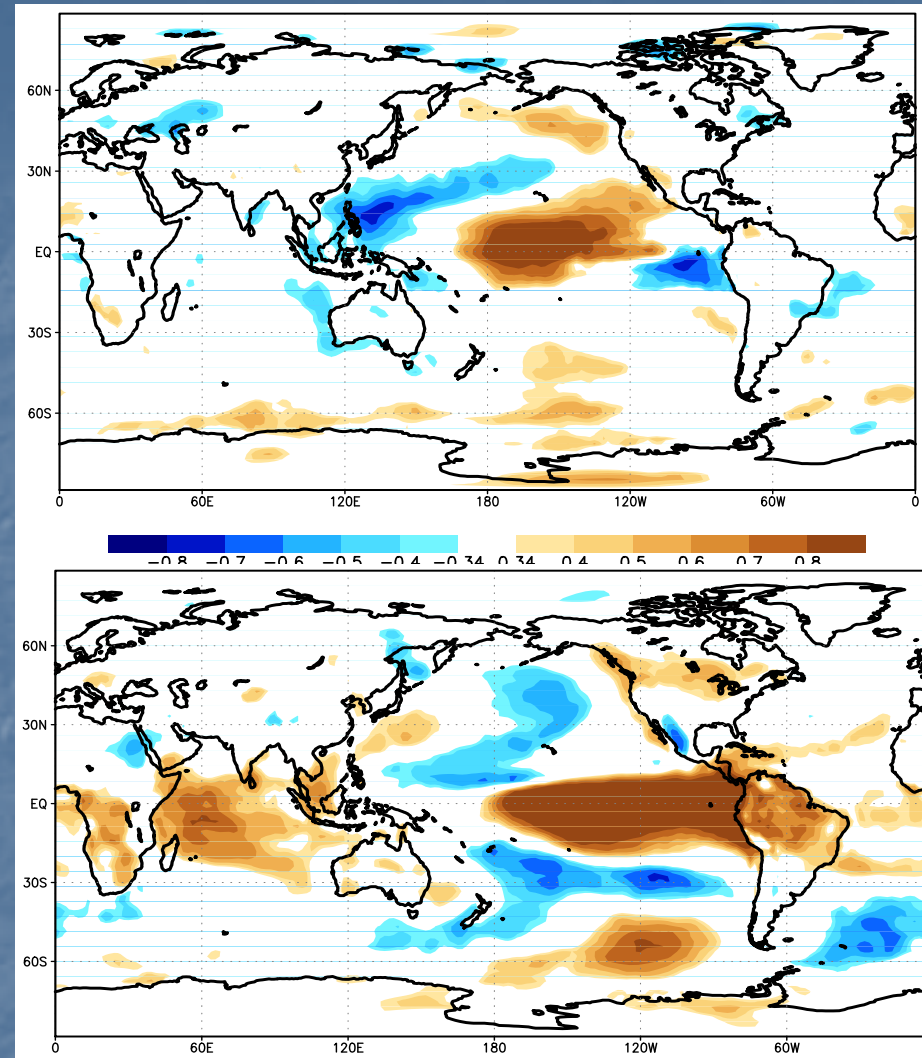
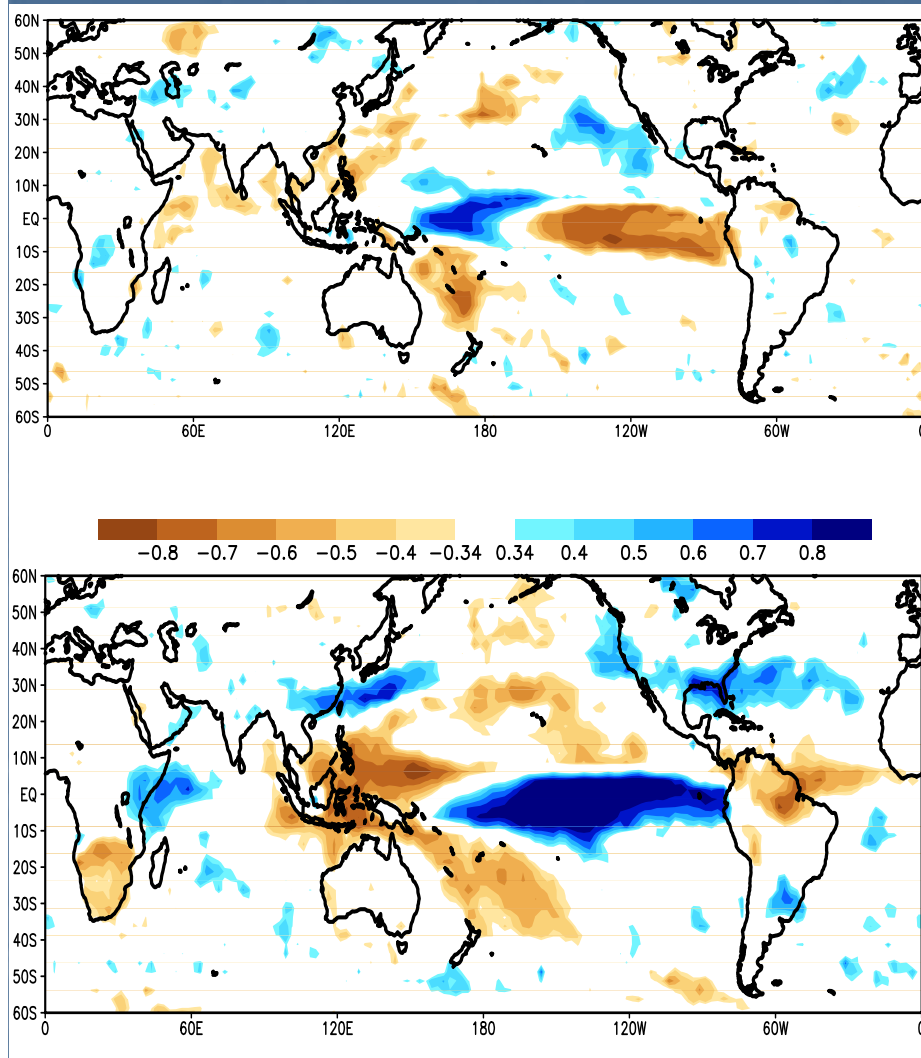
IODMI





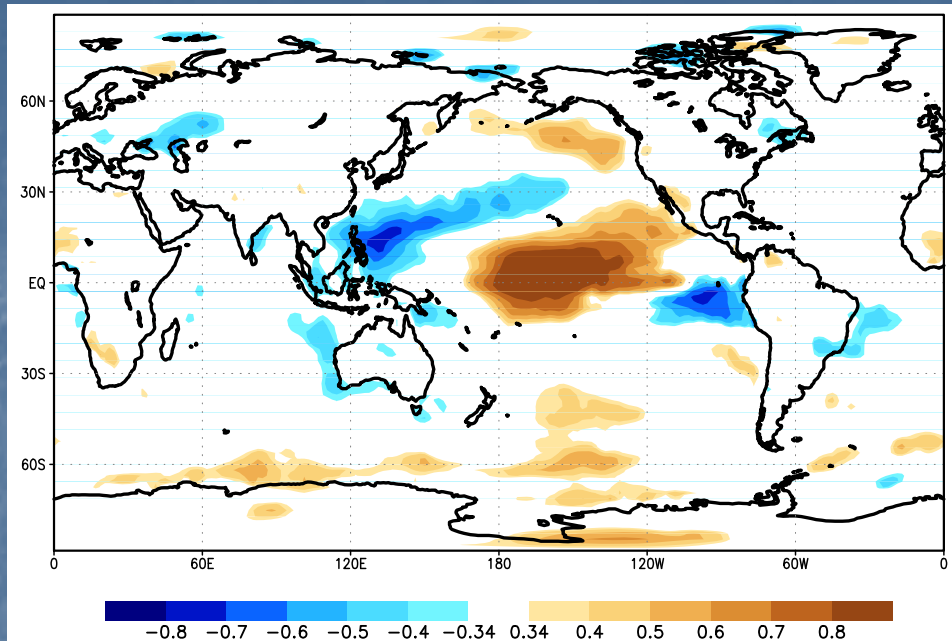
**Fig.** DJF (1979-2004) partial correlations between Rainfall anomalies and EMI (top) and NINO3 index (right). Shaded values are significant at 90% confidence level from a two tailed Student's t-test.



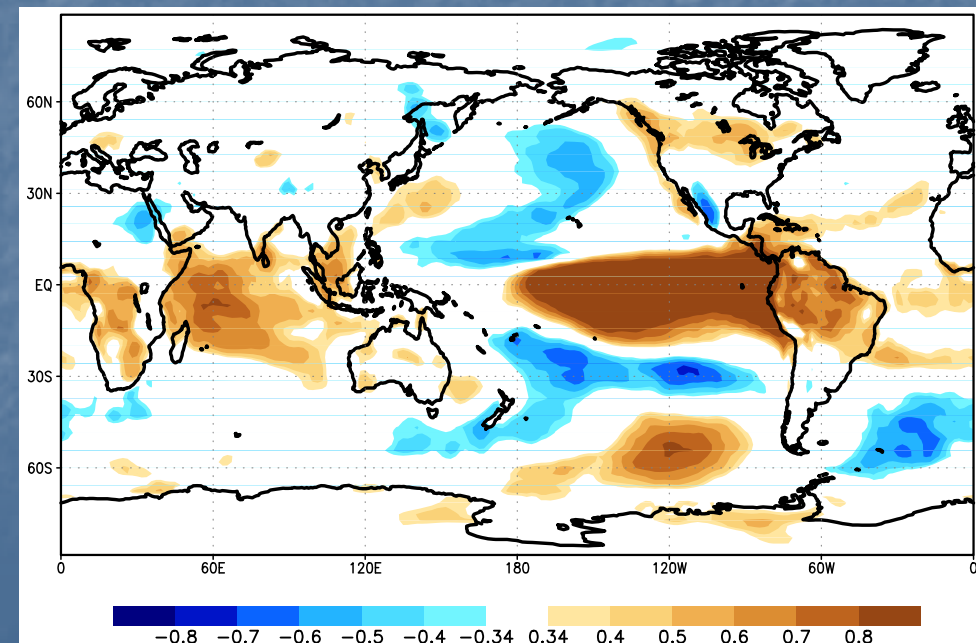


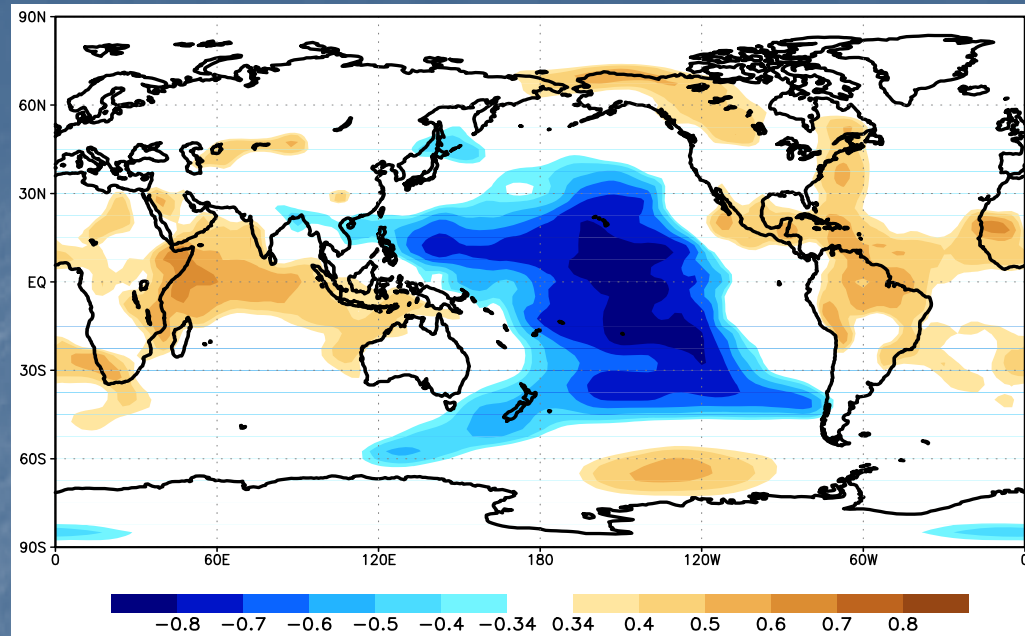
**Fig. DJF (1979-2004) partial correlations between**  
 Rainfall anomalies and EMI (Left top)  
 Rainfall anomalies and NINO3 index (Left Bottom)  
 temperature (2m height) anomalies and EMI (Right top)  
 temperature (2m height) anomalies and EMI (Right Bottom)

Shaded values are significant at 90% confidence level from a two tailed Student's t-test.

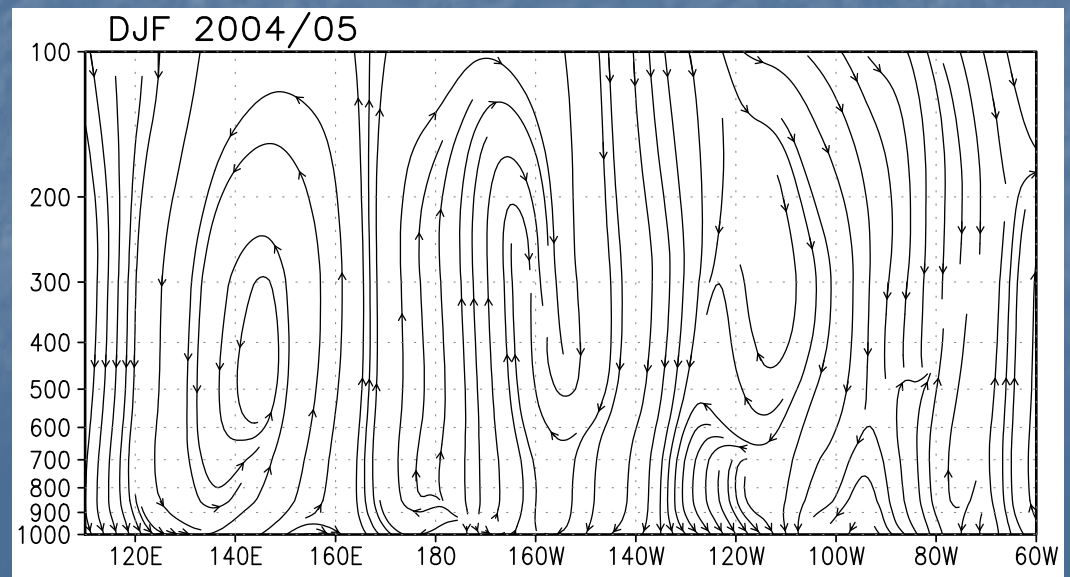


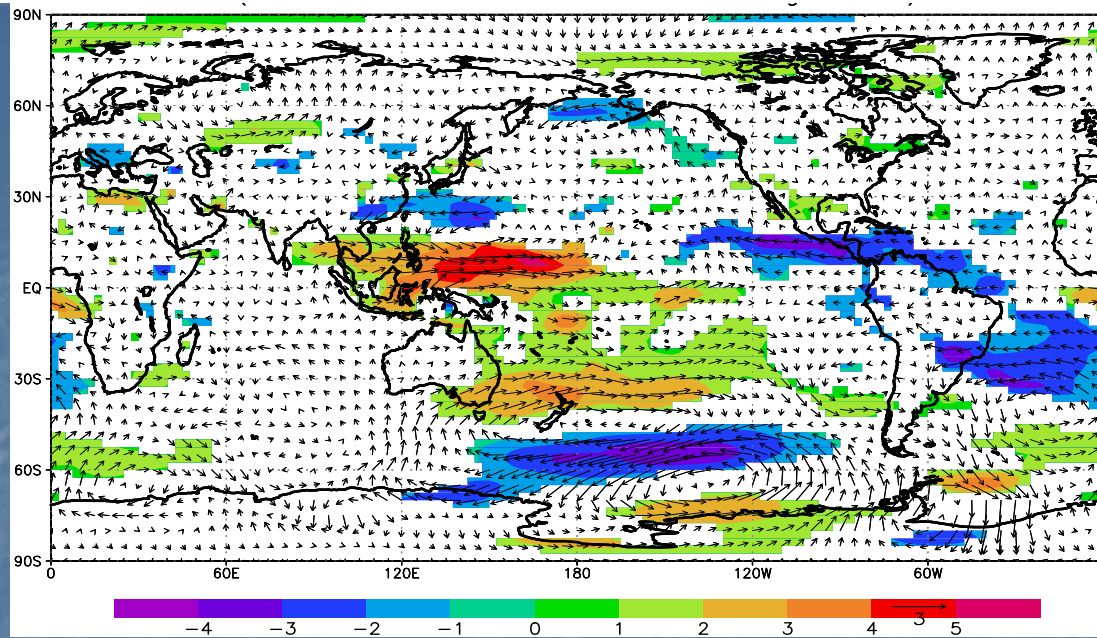
**Fig.** DJF (1979-2004) partial correlations between temperature (2m height) anomalies and EMI (top) and NINO3 index (right). Shaded values are significant at 90% confidence level from a two tailed Student's t-test.



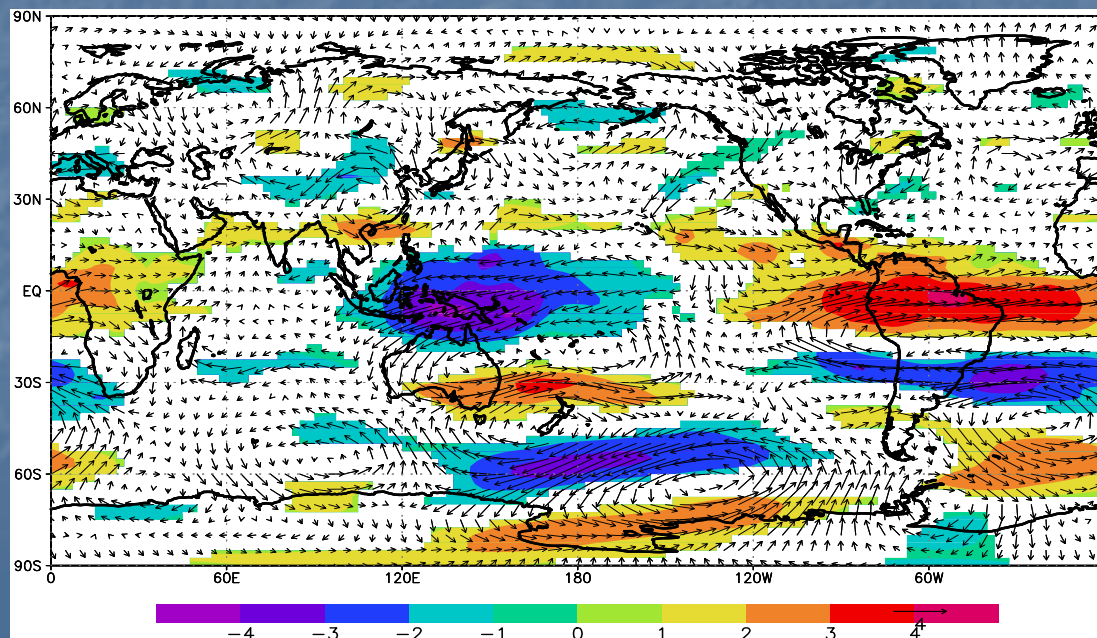


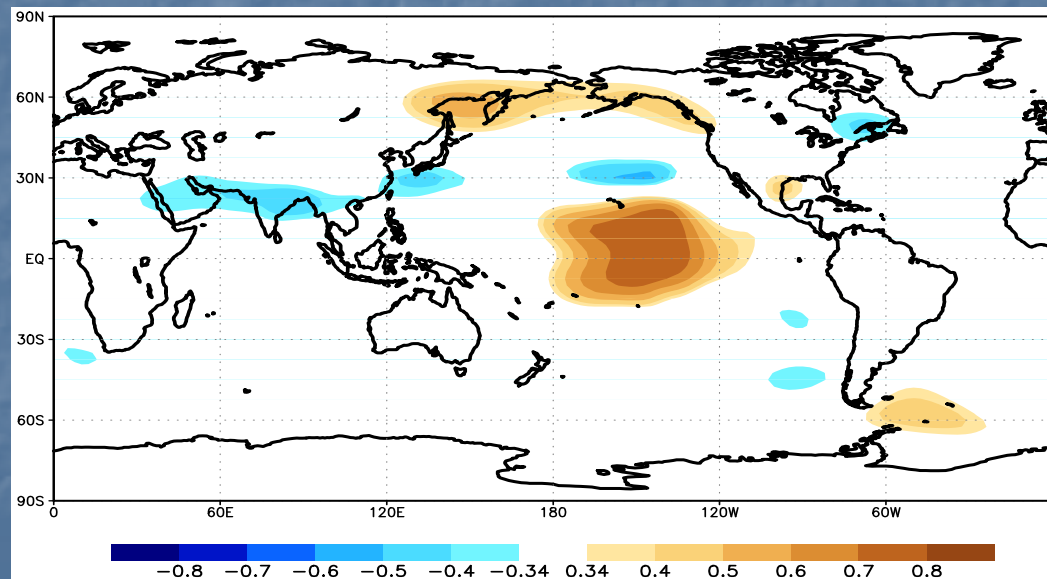
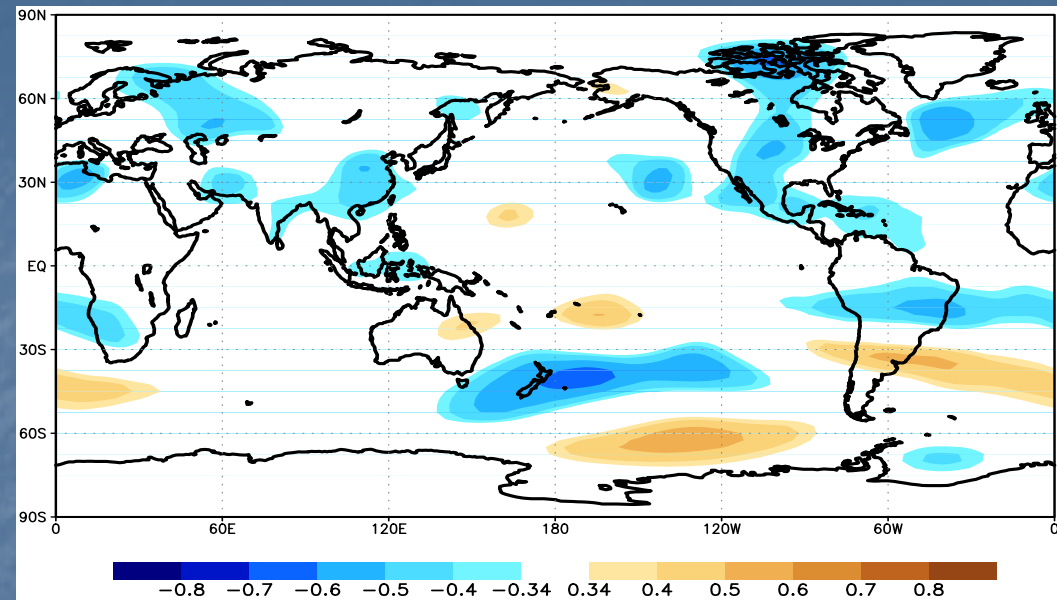
(Top): partial correlations between SLPA and EMI. (bottom): Walker circulation anoms, DJF 2004/05



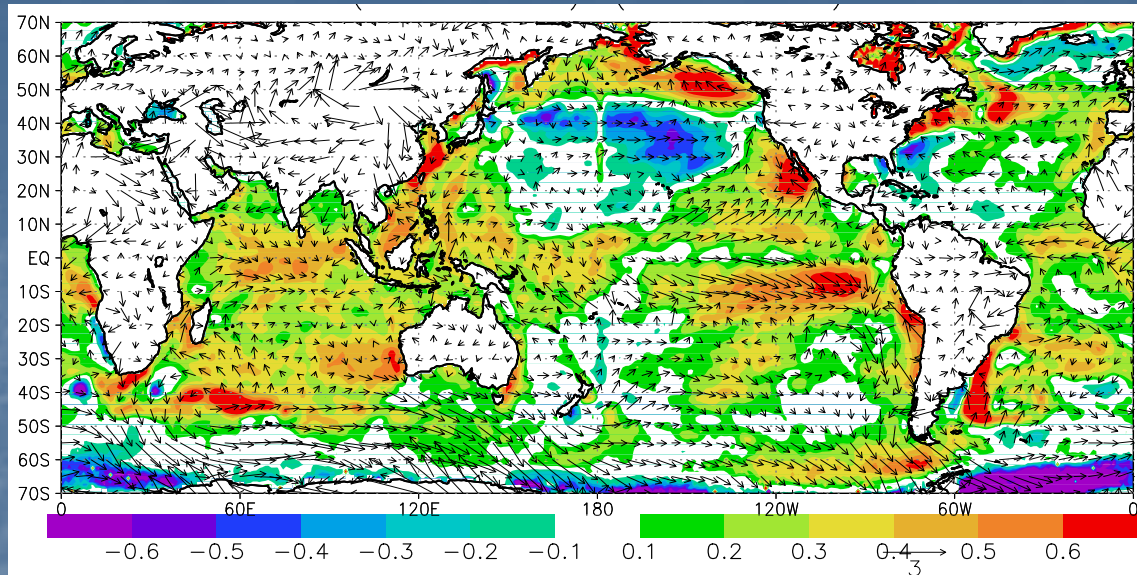


Composite JJAS anomalous winds obtained from seven strong El Niño Modoki events at 850 hPa (top) and 200 hPa (bottom).

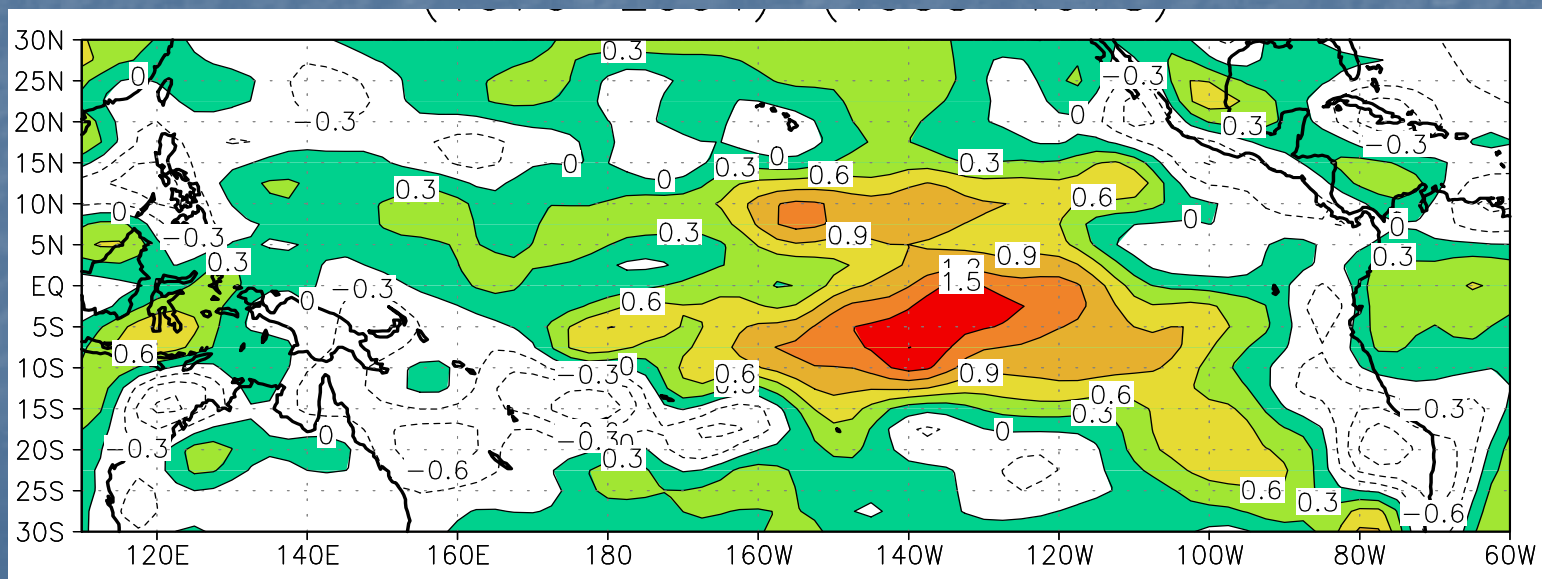




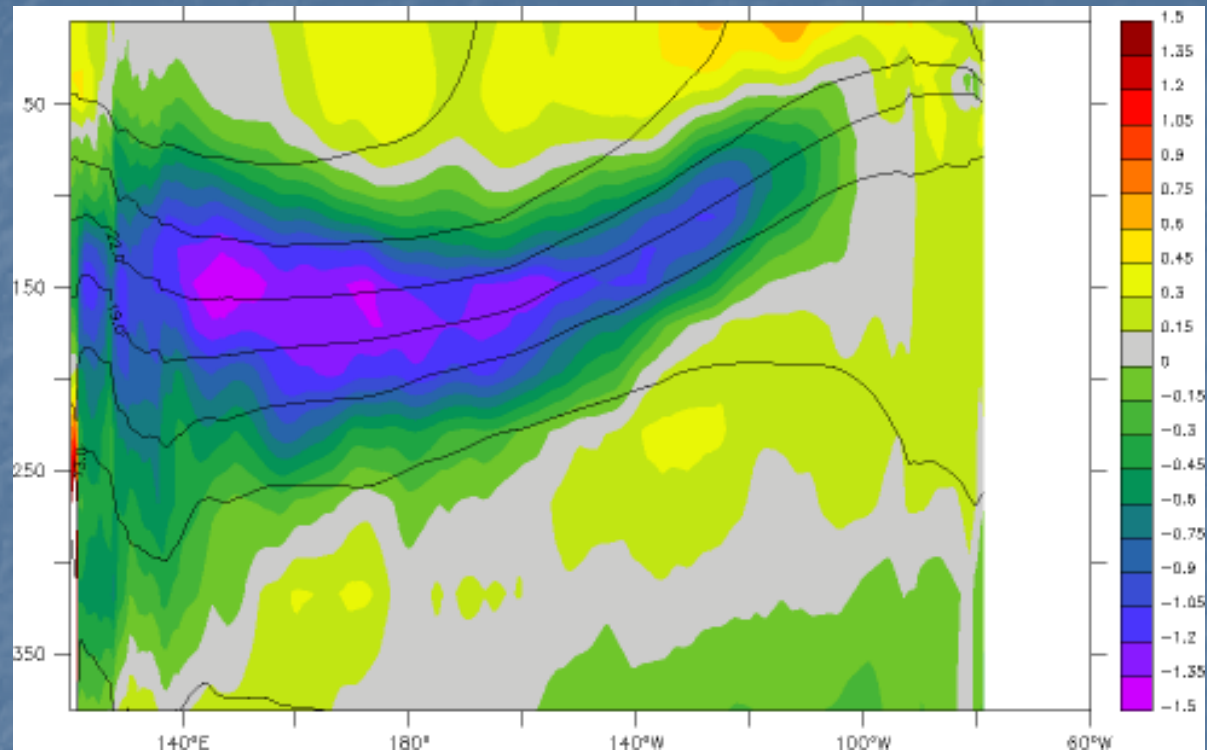
JJAS (1979-2004) partial correlations between 200 hPa geopotential anomalies and EMI (top) for JJAS (b) for DJF. Shaded values are significant at 90% confidence level from a two tailed Student's t-test.



Long-term changes in mean SST (°C) and winds at 1000 hPa (m/s), obtained by subtracting the mean SST of the period 1958-1978 from that over the period 1979-2004.

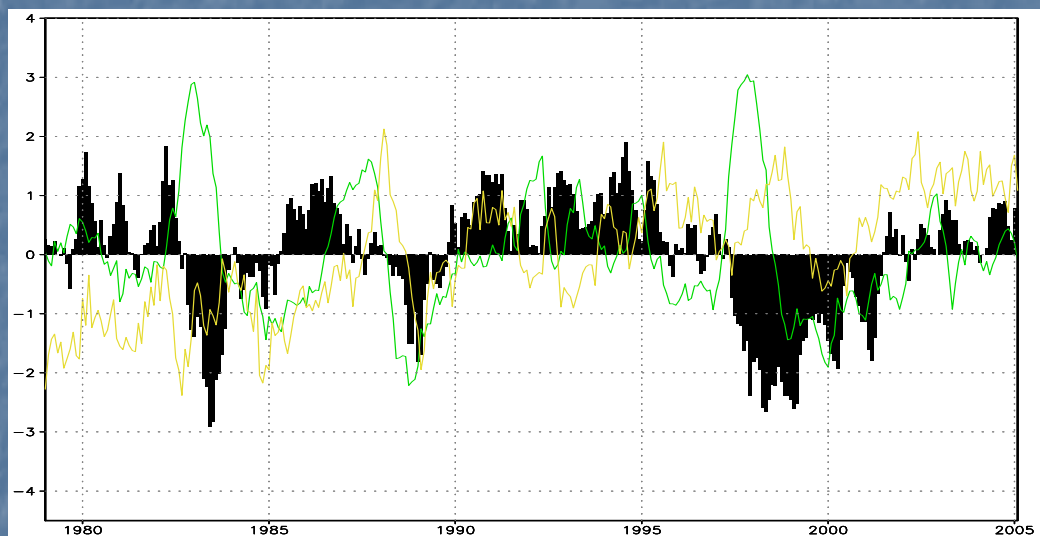
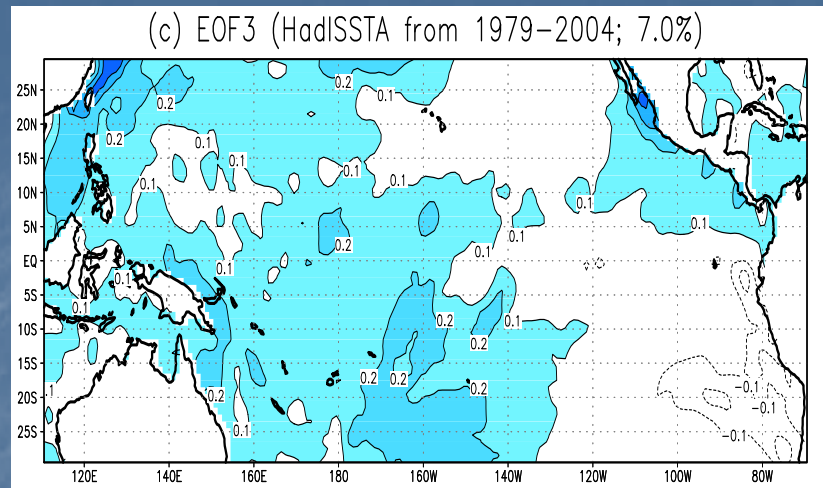


Long term changes in annual mean zonal winds at 1000 hPa (m/s), obtained as in Fig. 16a.



Differences of ocean temperature in two periods of 1958-78 and 1978-2004 along with the depth-longitude section of climatological ocean temperature (black contours).

\*\*Other possible causes also need to be explored.



Top left contributions from EOF2 during JJA 2004 obtained by multiplying the EOF2 with seasonal average of PC2 for JJA 2004,  
 Top right : (b) same as in (a) but from EOF3.  
 Bottom: Pc1 (green), PC2 (Bar), and PC3 (Yellow)

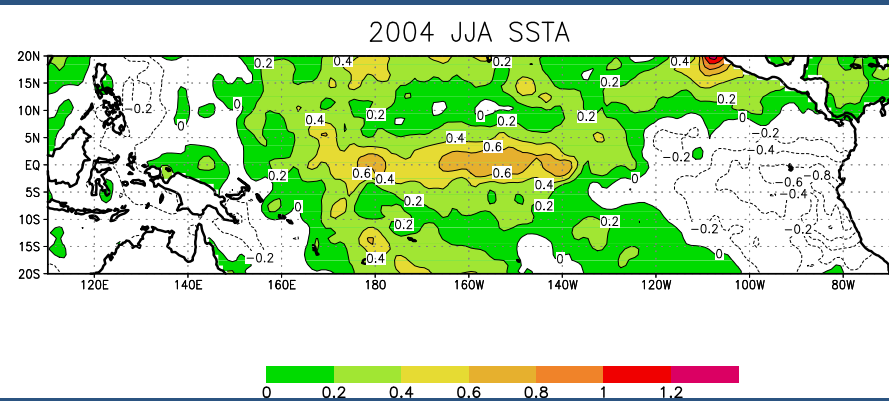
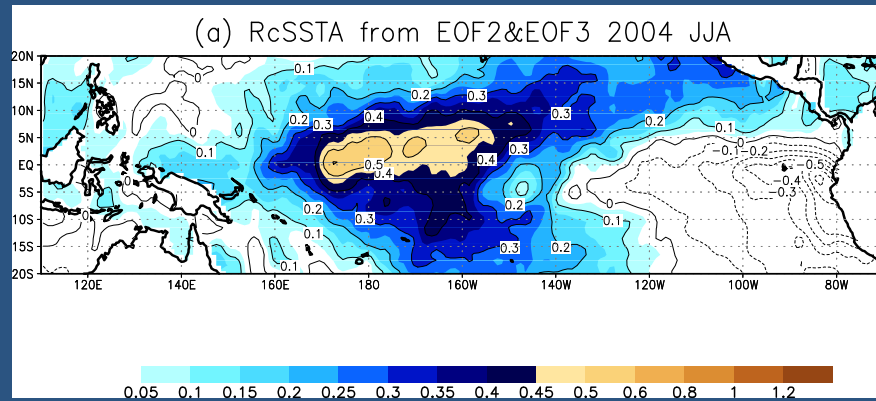
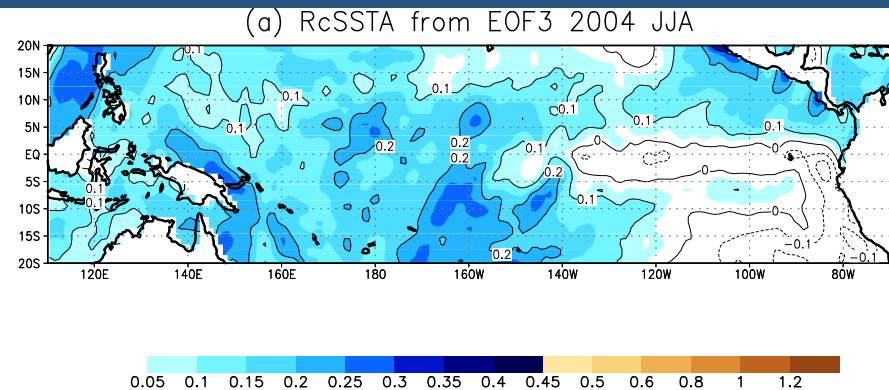
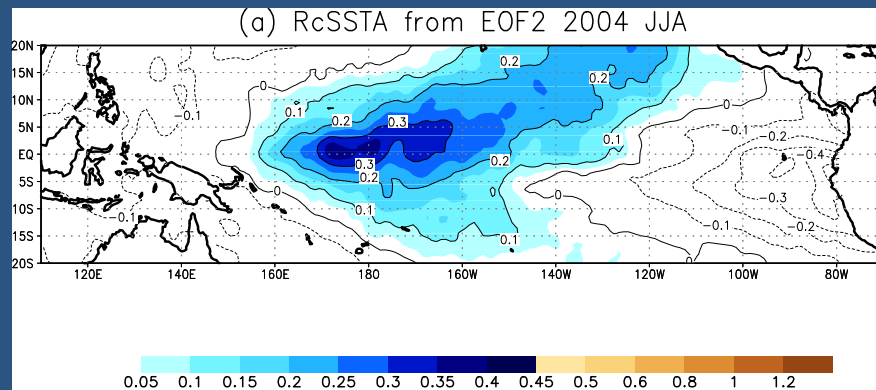
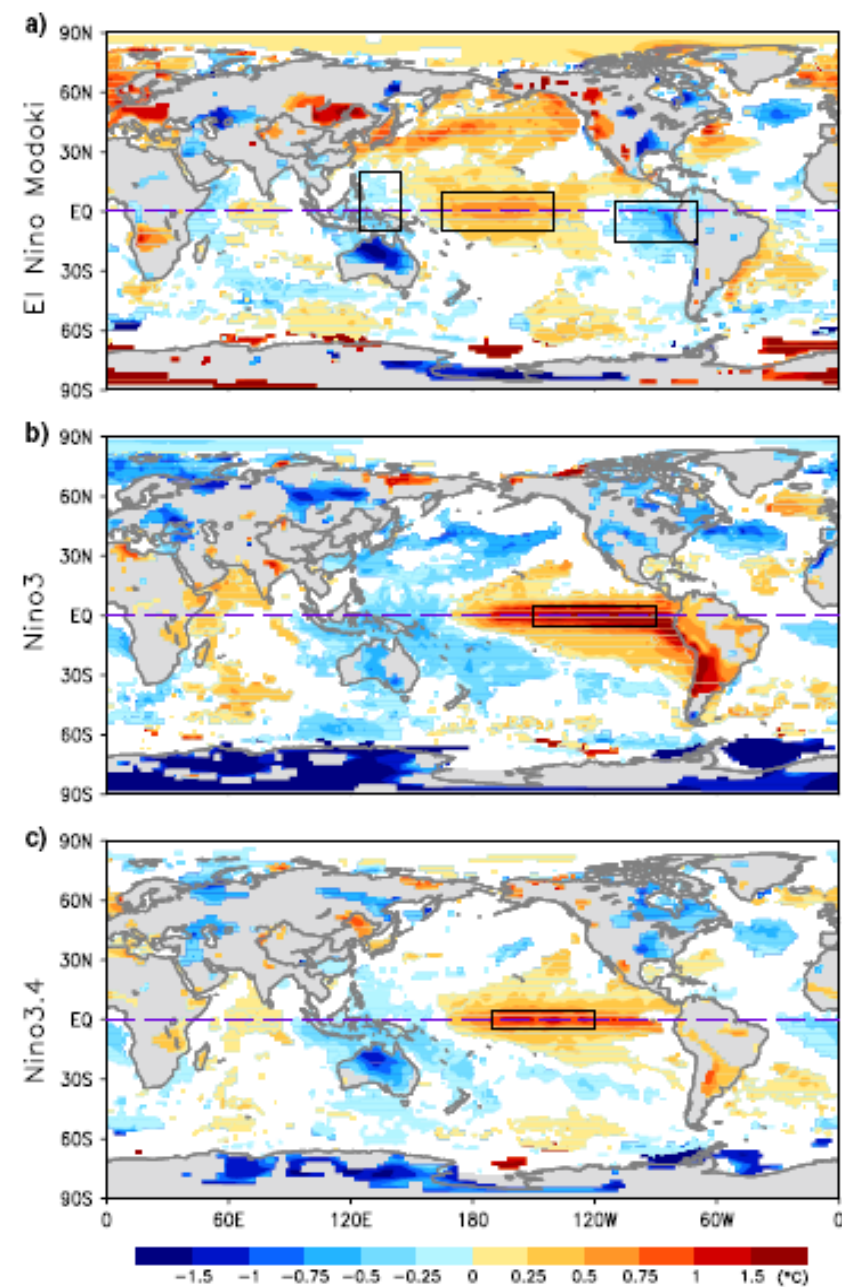


Figure: (a) contributions from EOF2 during JJA 2004 obtained by multiplying the EOF2 with seasonal average of PC2 for JJA 2004, (b) same as in (a) but from EOF3, (c) combined contributions from EOF2 and EOF3 during JJA 2004, (d) observed SSTA during JJA 2004

# Need for the appropriate index



# Summary

- ENSO Modoki is a unique coupled phenomenon of tropical Pacific, distinctly different and independent from ENSO as seen from the different evolution and teleconnection characteristics.
- We propose that the ENSO and ENSO Modoki are the top two modes of the coupled tropical Pacific system. The system chooses either of them, among other things, depending on the background conditions.
- Limitations: Linear analysis and data quality

# Acknowledgements

- *The senior author (TY) is encouraged by Mr. M. Yamamoto, a reporter of Kyodo News, to develop the present concept of ENSO Modoki in the early summer of 2004.*
- *The authors acknowledge Dr. Gary Myers for the discussion on Australian droughts, and Dr. J-J. Luo for discussion on the decadal changes in the tropical Pacific. Drs. R. Lucas, J. McCreary, S. Manabe, Z. Liu, H. Annamalai and T. Tozuka are also thanked for their suggestions and comments on an earlier version.*

# Future Plans/Scope

- Potential role of global warming in frequent occurrence of persistent ENSO Modoki
- Theoretical aspects of evolution
- Simulations in coupled models
- Predictability
- AGCM experiments.

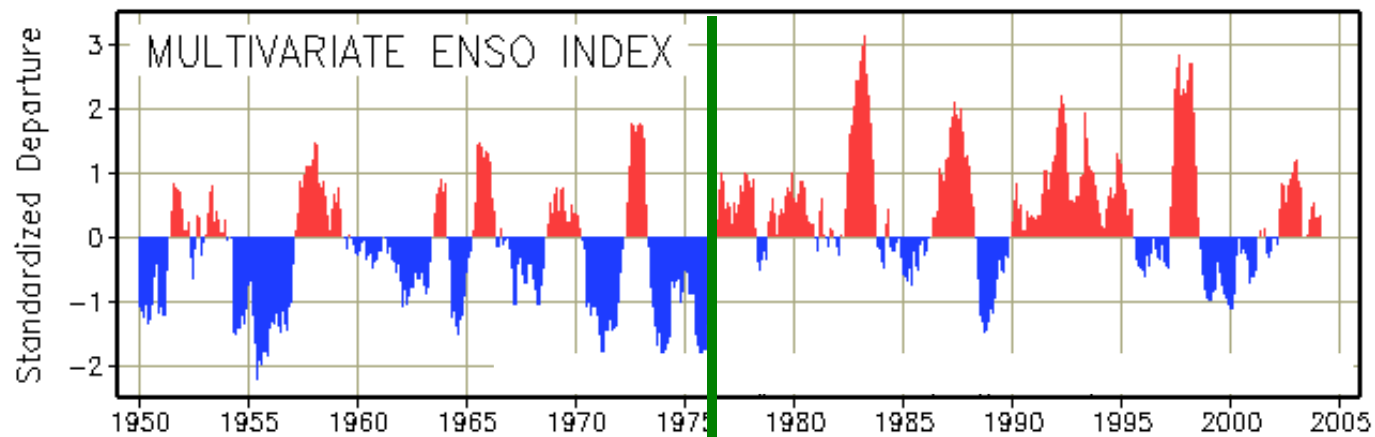
# Thank You

This paper is in Press with JGR-Oceans, and is available on line  
at <http://www.jamstec.go.jp/frsgc/research/d1/modoki/>

# Impact of Indian Ocean SST on developing El Niño

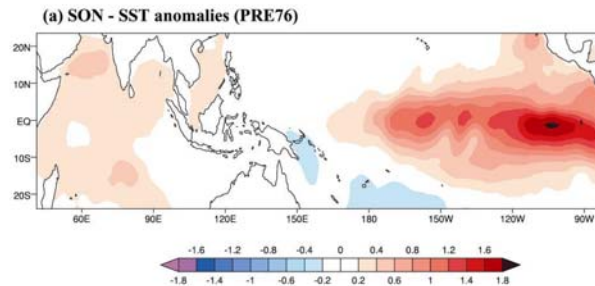
Annamalai et al., J. Climate, 2005

## Indian Ocean on the Intensity of El Nino?

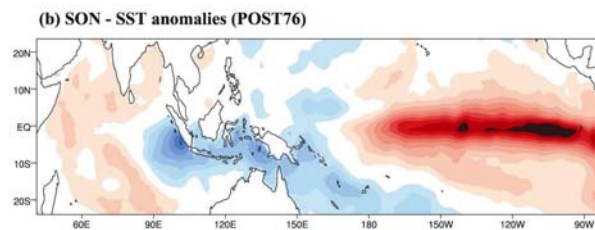


**PRE76**

**POST76**



**PRE76**



**POST76**

**Air-sea interaction along the equatorial IO peaks in SON -**

**Exclusive effect of IO SST**

# Experimental Designs

**(i) Tropical Indo-Pacific (TIP)**

**(ii) Tropical Pacific only (TPO)**

**(iii) Tropical Indian Ocean (TIO)**

**10 member ensemble; Two years covering the entire life-cycle of**

**El Nino (YEAR (0) to YEAR (+1))**

**ECHAM5.1 (MPI) – T42**

# ECHAM5 Climatology

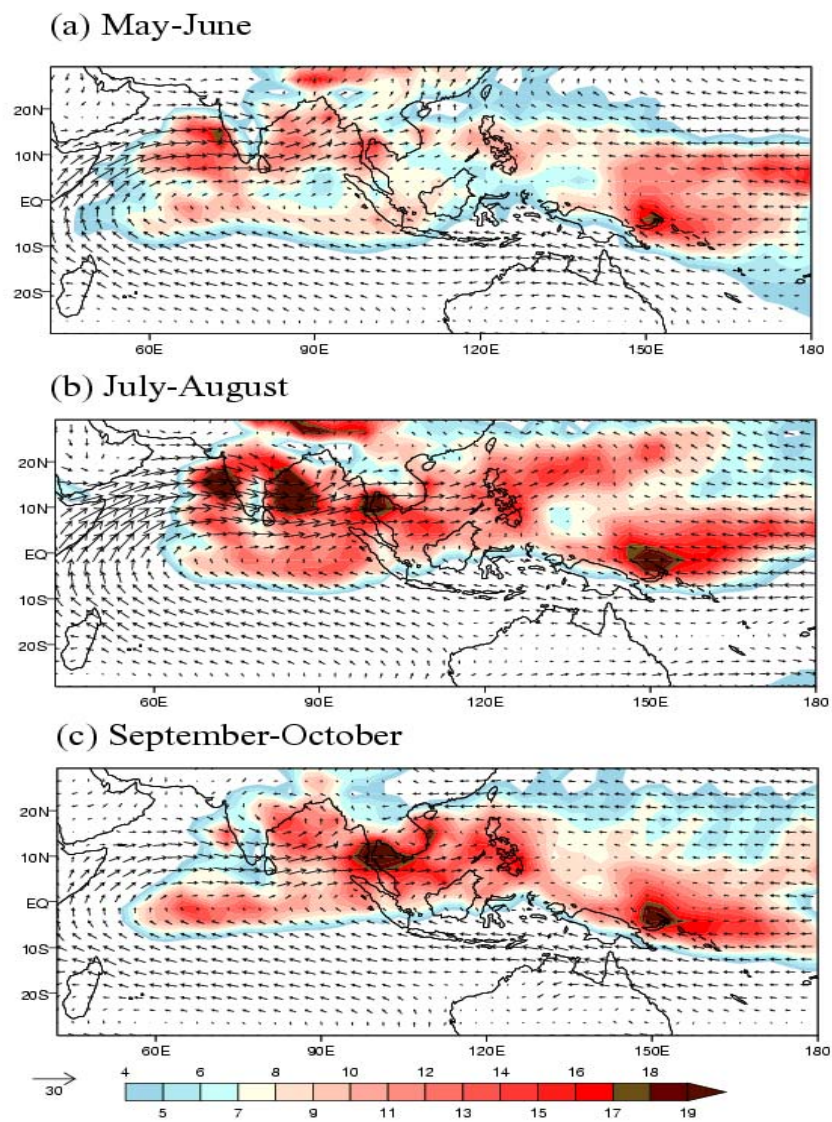
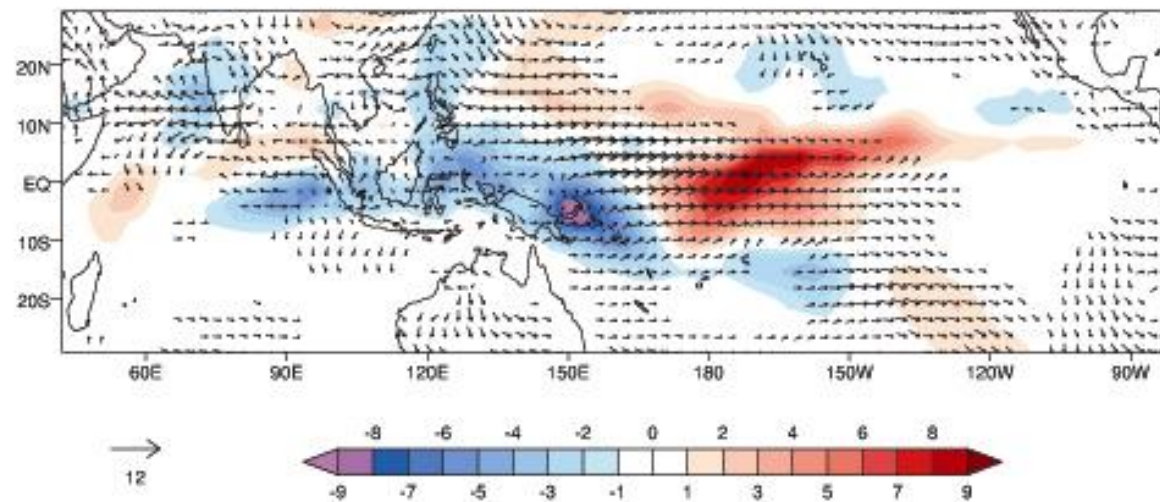


Figure 8: Same as Figure 3 but for the ECHAM5 AGCM.

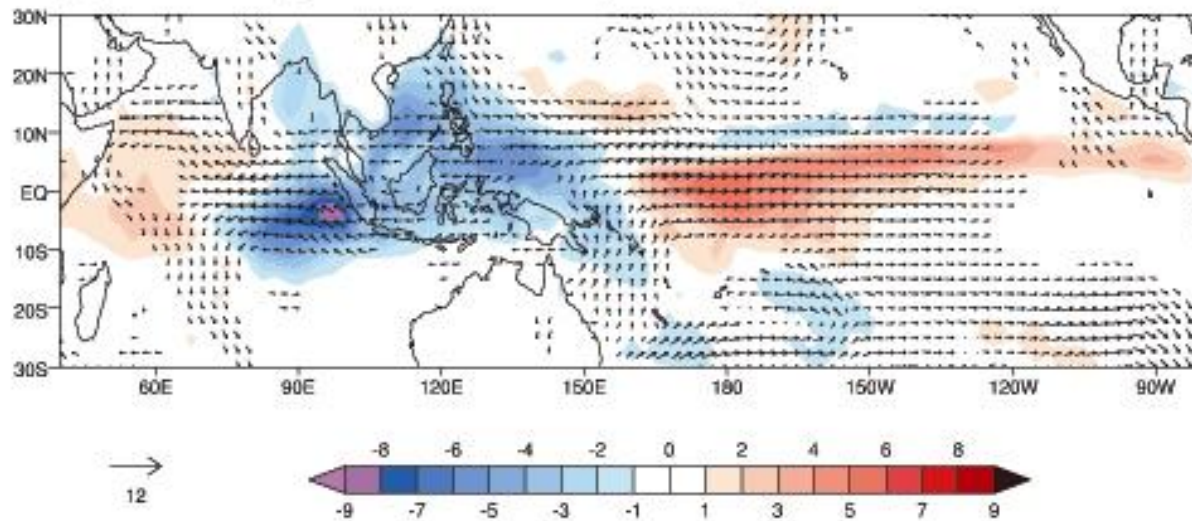
AGCM

(a) SON - Precipitation and 850 hPa wind anomalies (TIP\_POST)



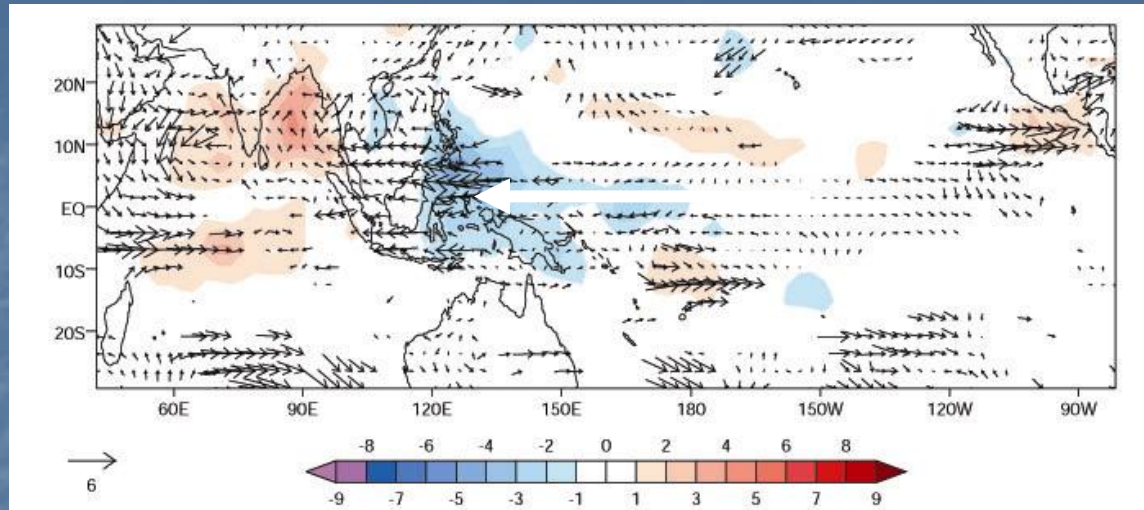
Obs

(b) SON - Precip. and 850hPa wind (POST76)



## TIP minus TPO

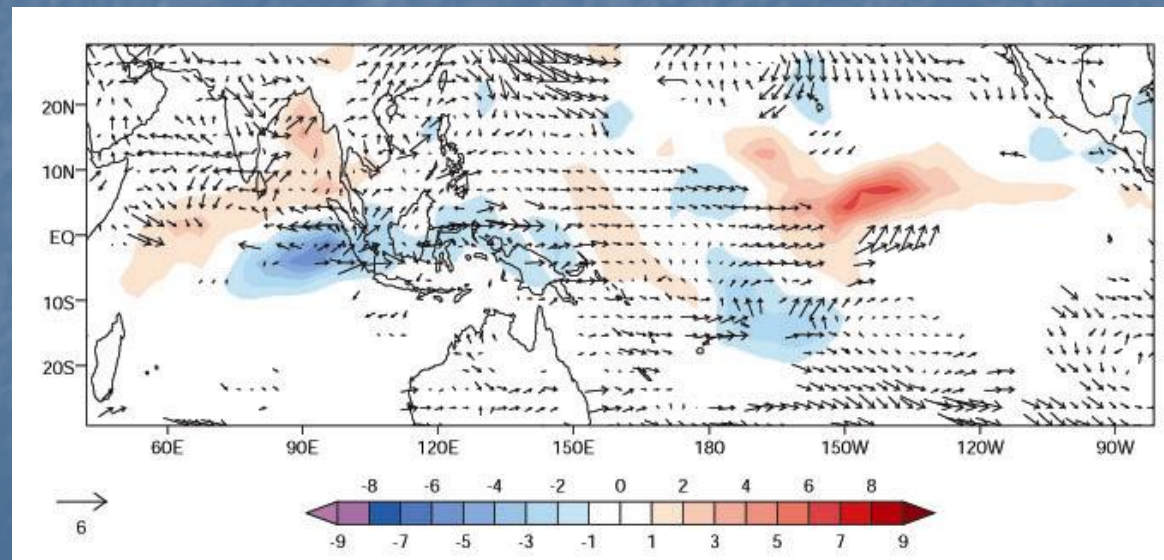
PRE - 76



Linear  
Response

## TIP minus TPO

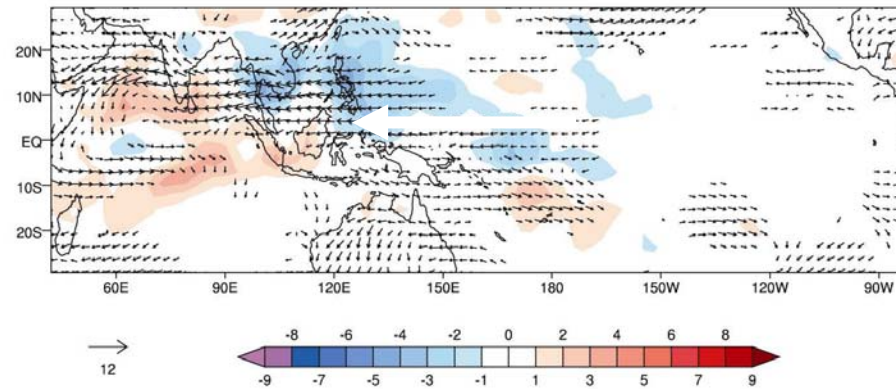
POST - 76



# TIO – Solutions

PRE – 76

(a) SON - Precipitation and 850 hPa wind anomalies (TIO\_PRE)



Non-local  
effects

POST – 76

(b) SON - Precipitation and 850 hPa wind anomalies (TIO\_POST)

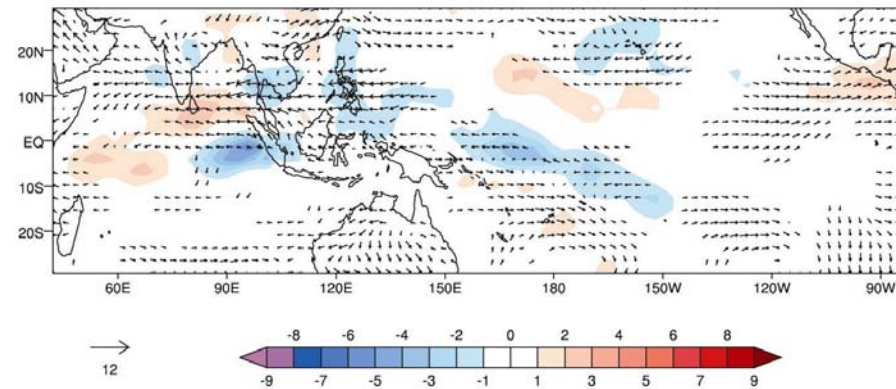
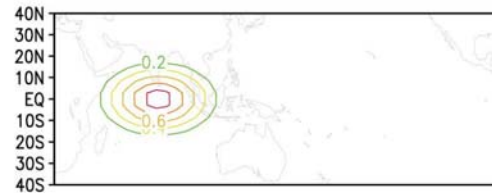


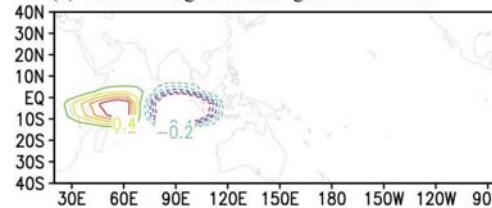
Figure 9: Same as Fig. 6 but for the Tropical Indian Ocean (TIO) runs.

## Linear Atmospheric Model – Watanabe

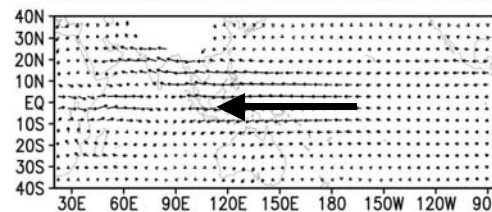
(a) Column integrated heating for basin-wide warming



(b) Column integrated heating for IOD/IOZM

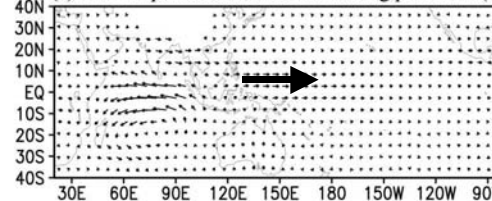


(c) wind response at 850 hPa for heating pattern in (a)



**Weakens El Nino  
Induced Westerlies**

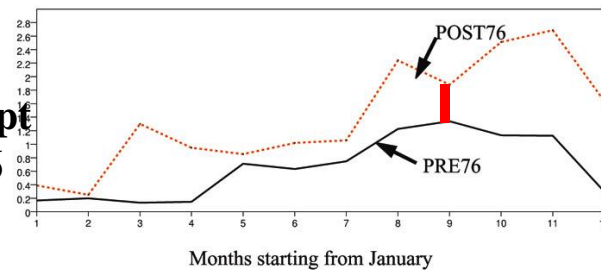
(c) wind response at 850 hPa for heating pattern in (b)



**Strengthens El Nino  
Forced Westerlies**

### 850 hPa winds – Eq. Central Pacific

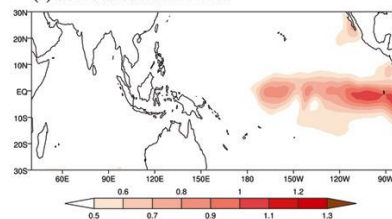
**Intensifies in Sept  
During POST76**



**Decreases in Nov.**

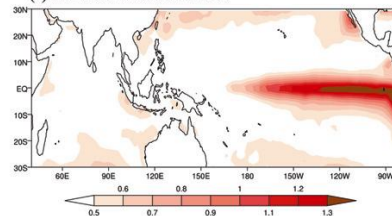
**Decreases in Sept.**

(b) SST r.m.s variance PRE76



**PRE76**

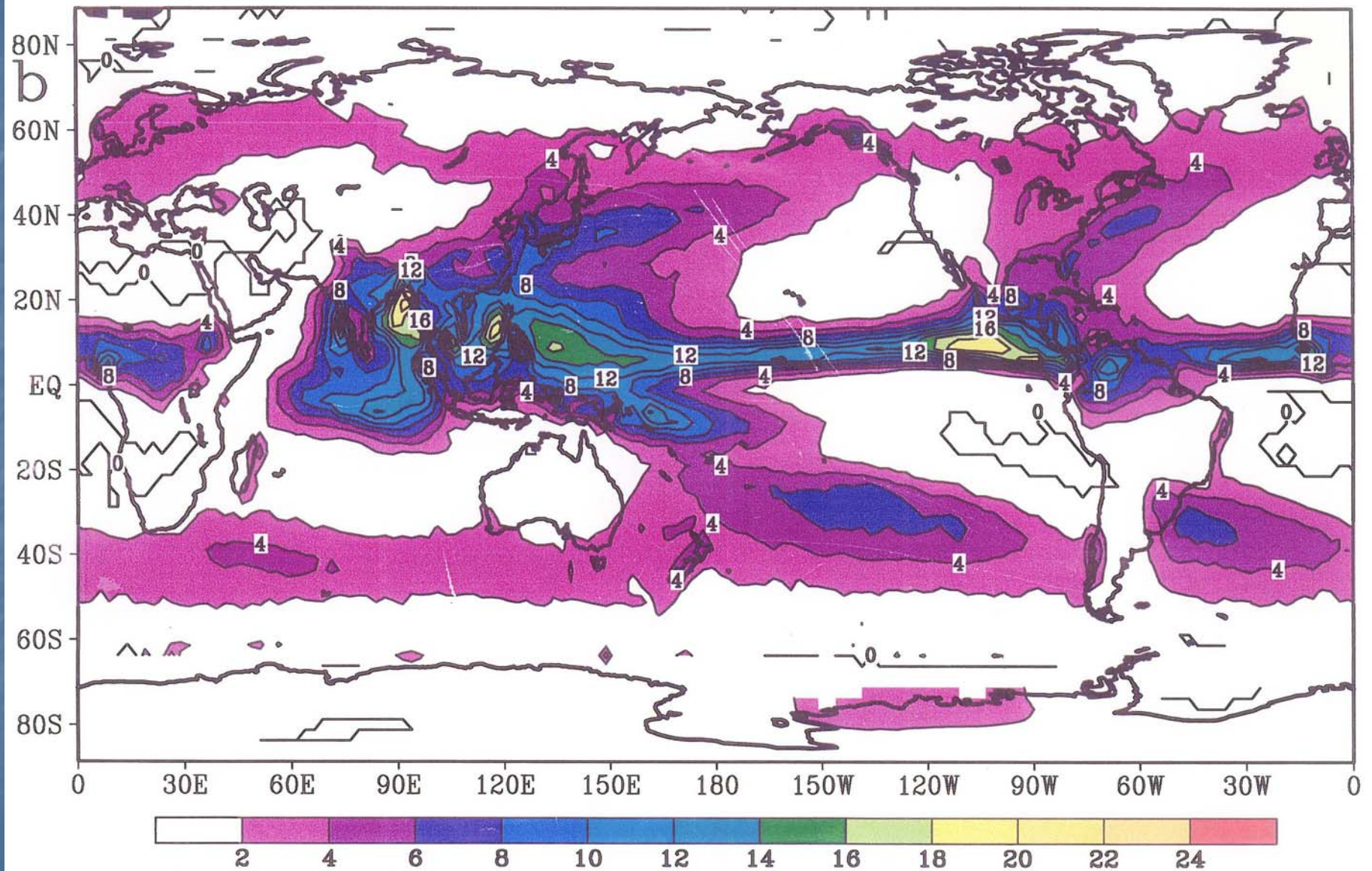
(c) SST r.m.s variance POST76



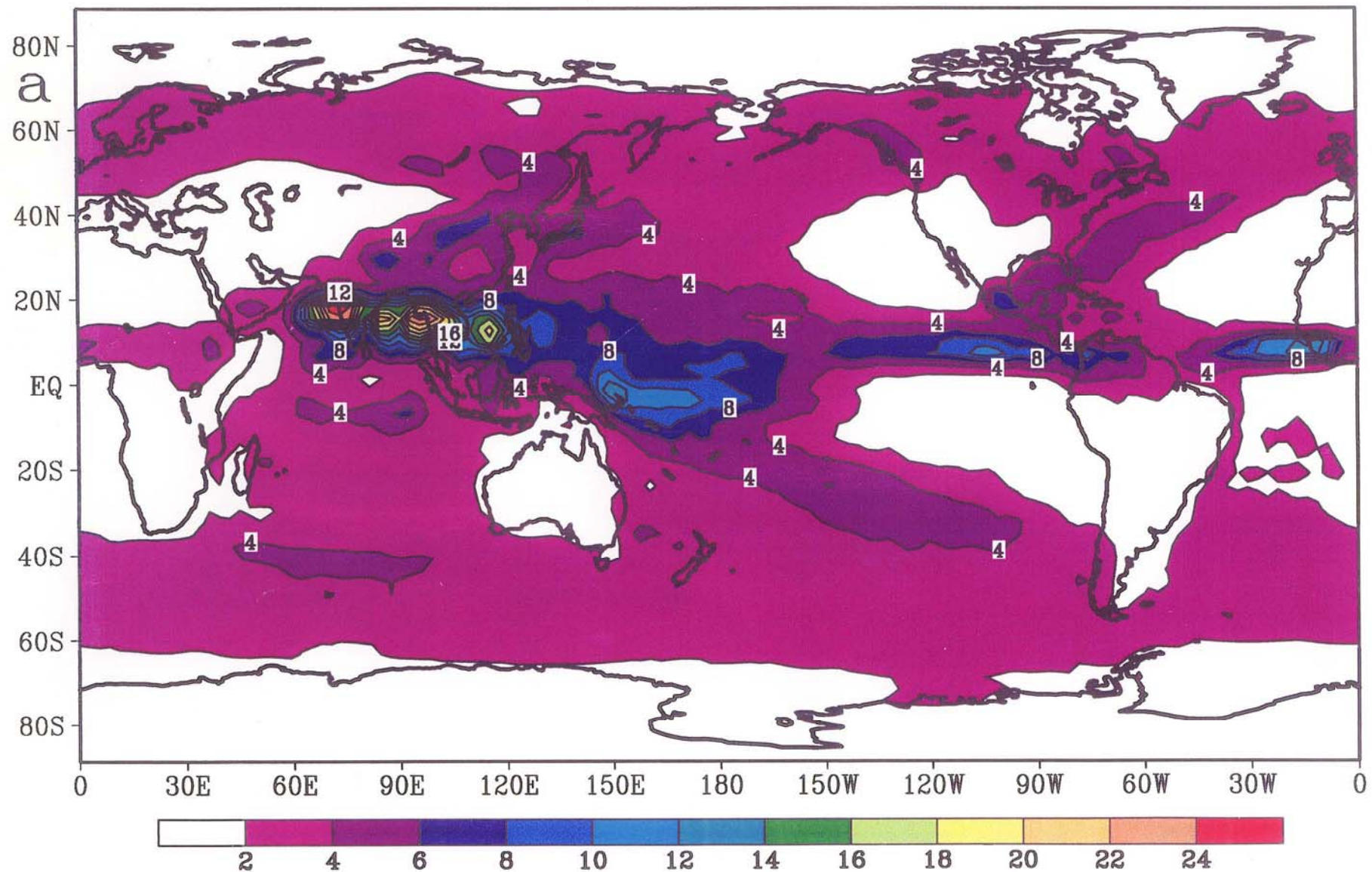
**POST76**

# Multiple convection

# Rainfall JJAS M.(CMAP 1979–1997 M.CLIM.)



# Rainfall JJAS M.(T42L28 1979-1997 M.CLIM.)



Simulated Mean JJAS Precipitation (mm/day)  
(10-yr clim. twin conv.)

